

**STUDY OF WEB STRUCTURE USING
STRAIN MEASUREMENTS**

By

SREERAM KRISHNA

Bachelor of Science

RV College of Engineering

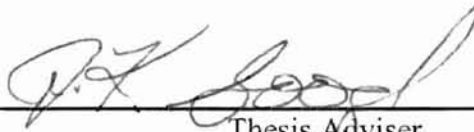
Bangalore, India

1997

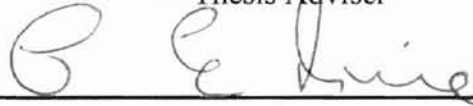
Submitted to the Faculty of the
Graduate College of the
Oklahoma State University
in partial fulfillment of
the requirements for
the Degree of
MASTER OF SCIENCE
December 2000

STUDY OF WEB STRUCTURE USING
STRAIN MEASUREMENTS

Thesis Approved:



Thesis Adviser







Dean of the Graduate College

ACKNOWLEDGEMENT

I would like to express my deepest gratitude to my advisor, Dr. J.K. Good for supporting me and for guiding me throughout this project. I would like to thank WHRC senior research engineer, Mr. Ron Markum, for his constant help in everything from the beginning.

I would like to thank my committee members Dr. Price and Dr. Lu for providing all the necessary guidance and assistance. I would like to thank my project associates, Balaji, Karthik, John, Joe and all my friends who directly or indirectly helped me to complete my thesis.

An acknowledgement would be incomplete if it is not bestowed towards my parents, my brother and my family members without whose support and scrupulous supervision, none of this would have been possible. I would finally like to thank the sponsors of my project and the school of Mechanical and Aerospace Engineering, OSU, for such a wonderful experience.

TABLE OF CONTENTS

Chapter	Page
I. INTRODUCTION	1
1.1 Web	1
1.2 Web Handling	1
1.3 Types Of Winding.....	3
1.4 Roll-Structure Measurement Techniques.....	3
II. LITERATURE REVIEW	6
2.1 Impacters	6
2.1.1 Schmidt Hammer.....	7
2.1.2 Rho-Meter	8
2.1.3 Paro tester.....	9
2.2 Stress And Strain.....	10
2.2.1 Cameron Gap Test.....	10
2.2.2 J-Line Test.....	11
2.2.3 Strain Gages	12
2.3 Interlayer Pressure.....	13
2.3.1 Pull-Tabs	14
2.3.2 Smith Roll-Tightness Tester (Smith Needle).....	15
2.3.3 Force Sensing Resistor.....	16

Chapter	Page
2.3.4 Capacitance Gages	17
2.4 Density	18
2.5 Other Methods.....	20
2.6 Theoretical Hakiel Model.....	20
2.7 Summary and Research Objective	22
III EXPERIMENTAL PROCEDURE	24
3.1 Experimental Procedure	25
3.2 Theoretical Model	26
3.2.1 Radial Modulus	26
3.2.2 Tangential Modulus.....	27
3.2.2.1 Stretch Test.....	27
3.3 Pressure Measurement.....	32
3.3.1 Calibration Of FSR.....	33
3.3.1.1 Loading Routine	33
3.3.2 Calibration Of Pull-Tabs	35
3.4 Winding.....	36
3.5 Experimental Procedure	38
3.5.1 Tabs	39
3.6 Strain Measurement.....	41
3.7 Resolution And Limitations	42
3.8 Resolution Obtained.....	43

Chapter	Page
IV. RESULTS	45
4.1 LDPE Wound At 100 psi Tension.....	45
4.2 Pressure Comparison Using Pull-Tabs.....	48
4.3 Pressure Comparison Using FSR.....	50
4.4 LDPE Wound At 200 psi Tension.....	52
4.5 Pressure Comparison Using FSR at 200 psi Web Tension	53
4.6 Non-Woven Material	54
4.7 Pull-Tab Calibration For Non-woven Material.....	55
4.8 Pressure Comparison For Non-woven Material.....	56
4.9 Comparison Of Strains For Non-woven Material	58
V. CONCLUSIONS	59
VI. FUTURE WORK	61
6.1 Strain Measurement With Potentiometer.....	61
6.2 Calibration.....	64
6.3 Tabs.....	65
REFERENCES	67
APPENDIX	70

LIST OF TABLES

Table	Page
3.1 Inputs To The Winder software for LDPE.....	30
3.2 Inputs To The Winder software for Non-woven.....	31
3.3 Resolution of the Method.....	44
4.1 Error in measurements by vernier near the core	46
4.2 Error analysis of Strains (LDPE, 100 Psi).....	47
4.3 Error Analysis of Pressures using Pull-tabs (LDPE, 100 psi).....	49
4.4 Error Analysis of pressures using FSRs (LDPE, 100 psi).....	51
4.5 Error Analysis of strains (LDPE, 200 psi)	52
4.6 Error analysis of pressures using FSRs (LDPE, 200 psi).....	54
4.7 Error analysis of pressures (Non-woven, 71.89 psi)	57
4.8 Error analysis of strains (Non-woven, 71.89 psi).....	58
A-1 Error analysis of Strains (LDPE, 100 Psi web tension)	73
A-2 Error analysis of pull-tab readings (LDPE, 100 psi, Trial 1).....	75
A-3 Error analysis for Pull-tabs stresses (LDPE, 100 psi, Trial 2)	76
A-4 Error analysis of Pull-tab stresses (LDPE, 100 psi, Trial 3).....	77
A-5 Error Analysis of Pull-tab Pressures (LDPE, 100 psi).....	78
A-6 Error analysis for three FSR trials (LDPE, 100 psi)	81
A-7 Error Analysis of three Strains (LDPE, 200 Psi)	84
A-8 Error analysis of three FSR pressures (200 psi, LDPE).....	87
A-9 Error analysis on three strains (Non-woven, 71.89 psi).....	90
A-10 Comparison of stresses (Non-woven, 71.89 psi, Trial 1).....	92
A-11 Comparison of stresses (Non-woven, 71.89 psi, Trial 2).....	93
A-12 Comparison of stresses (Non-woven, 71.89 psi, Trial 3).....	94
A-13 Error analysis for Pull-tab stresses (Non-woven, 71.89 psi).....	95
A-14 Core Properties.....	96

Table	Page
A-15 Properties for the winder software for LDPE	96
A-15 Properties of Non-woven for Winder software	96

LIST OF FIGURES

Figure	Page
2.1 Schmidt Hammer.....	7
2.2 Rho-meter.....	9
2.3 Parotester.....	10
2.4 J-line test.....	12
2.5 Smith needle.....	16
2.6 Density Analyzer.....	19
3.1 Stress Vs Strain plot for LDPE obtained by stretch test.....	29
3.2 Maximum possible variation in strain due to E_R and E_T	32
3.3 Calibration of FSR (uploading).....	34
3.4 Pull-tab calibration (uploading).....	36
3.5 Experimental set up.....	37
3.6 Shim tabs and FSRs.....	41
4.1 Comparison of Strains (LDPE, 100 psi).....	47
4.2 Comparison of stresses using pull-tabs (LDPE, 100 psi).....	49
4.3 Comparison of stresses using FSR (LDPE, 100 psi).....	51
4.4 Comparison of strains (LDPE, 200 psi).....	52
4.5 Comparison of pressures using FSRs (LDPE, 200 psi).....	54
4.6 Pull-tab Calibration for non-woven material.....	55
4.7 Comparison of pressures using pull-tabs (Non-woven, 71.89 psi).....	57
4.8 Comparison of strains (Non-woven, 71.89 psi).....	58
6.1 Potentiometer setup.....	62
6.2 Circuit diagram of potentiometer set up.....	63
6.3 Calibration Of Potentiometer.....	64
A-1 Comparison of Strains (LDPE, 100 psi, Trial 1).....	71

Figure	Page
A-2 Comparison of Strains (LDPE, 100 psi, Trial 2).....	71
A-3 Comparison of Strains (LDPE, 100 psi, Trial 3).....	72
A-4 Error analysis on strain values (LDPE, 100 psi).....	73
A-5 Comparison of Stresses using Pull-tabs (LDPE, 100 psi, Trial 1).....	75
A-6 Comparison of Stresses using Pull-tabs (LDPE, 100 psi, Trial 2).....	76
A-7 Comparison of Stresses using Pull-tabs (LDPE, 100 psi, Trial 3).....	77
A-8 Error analysis on three pressures (LDPE, 100 psi).....	78
A-9 Comparison of Pressures using FSR (LDPE, 100 psi, Trial 1).....	79
A-10 Comparison of Pressures using FSR (LDPE, 100 psi, Trial 2).....	80
A-11 Comparison of Pressures using FSR (LDPE, 100 psi, Trial 3).....	80
A-12 Error Analysis of three FSR readings (LDPE, 100 psi).....	81
A-13 Comparison of Strains (LDPE, 200 psi, Trial 1).....	82
A-14 Comparison of Strains (LDPE, 200 psi, Trial 2).....	83
A-15 Comparison of Strains(LDPE, 200 psi, Trial 3).....	83
A-16 Error analysis of strains for three trials (LDPE, 200 psi).....	84
A-17 Comparison of Pressures (LDPE, 200 psi, Trial 1).....	85
A-18 Comparison of Pressures (LDPE, 200 psi, Trial 2).....	86
A-19 Comparison of pressures (LDPE, 200 psi, Trial 3).....	86
A-20 Comparison of pressures of three trials (LDPE, 200 psi).....	87
A-21 Comparison of strains (Non-woven, 71.89 psi, Trial 1).....	88
A-22 Comparison of Strains (Non-woven, 71.89 psi, Trial 2).....	89
A-23 Comparison of Strains (Non-woven, 71.89 psi, Trial 3).....	89
A-24 Error analysis on three strains (Non-woven, 71.89 psi).....	90
A-25 Comparison of stresses (Non-woven, 71.89 psi, Trial 1).....	92
A-26 Comparison of stresses (Non-woven, 71.89 psi, Trial 2).....	93
A-27 Comparison of stresses (Non-woven, 71.89 psi, Trial 3).....	94
A-28 Comparison of three stresses (Non-woven, 71.89 psi).....	95

Chapter 1

INTRODUCTION

1.1 Web

A web is a structure, which has length dimensions large compared to the proportions in the thickness and width directions. Webs are best defined as membranes whose in-plane stiffness far exceeds the bending stiffness. Common examples of webs that we come across in daily life are newspapers, plastic bags, and aluminum foil. Since webs find applications in copious forms from a common food wrapper to the more intricate sheets for a spacecraft, they need to be studied carefully.

1.2 Web Handling

Web behavior, in general, can be classified into four categories; longitudinal dynamics, lateral dynamics, winding/unwinding and wrinkling. In this thesis, we deal with the alteration in the structure of the web due to the stresses caused by winding.

Web handling involves the study of webs being wound and transported above a number of rollers where intermediate web processing operations like printing, in the case of newspapers may take place. In some cases, the roll is wound merely for transport from the manufacturing center to the processing center. The location, generally a shaft, at

which a web is 'unrolled' is called the unwind station and the location where the web is rolled back onto a rotating core is called the rewind station. The cores on which the web is wound play an important role in determining the stresses in the initial few layers of the wound roll. The wound roll must be tight enough to prevent telescoping (irregular winding resulting in the projecting of a few web layers beyond the wound plane) and collapsing during handling but not so compact that the material yields at the thick gage bands or such that the inner layers are buckled by the outer layers of material.

During winding, several parameters play a crucial role in determining the web structure such as the speed of the web being rolled, the web line tension (which is the tension at which the web is wound), and the wound on tension (WOT) which is the tension in the outer layer of a winding roll. The WOT can be influenced by the type of the winder (center or surface driven), web line tension (WLT), and the presence of the rider roll.

During winding, speed should be maintained within the limit at which air can get trapped in the web to produce defective rolls. The entrained air often leads to slippage related defects. An added complexity is that the web materials are often visco-elastic, which forces the winder operator to attempt not only to wind rolls that are defect free at the time of winding but to wind them such that they remain defect free until they have been converted into their final form.

1.3 Types Of Winding

There are basically two modes of winding on which are based all modern methods. They are center winding and surface winding. In this thesis the mode employed is center winding where a torque is input to the core of the winding roll.

1.4 Roll-Structure Measurement Techniques

Over the years, several methods have been adopted in the web handling industry to determine the roll-structure. The term 'roll-structure' is used to describe the condition of the wound roll. Pressures between the web layers have been measured using pull-tabs [18], the hardness of the exterior of the roll and the wound roll density have been used to attempt to quantify wound roll defects in terms of the measurement methods used and then input winder operating parameters that produce a roll-structure that is defect-free. The roll-structure measurements can be broadly classified into the following.

- 1) **Hardness Impacters** : The Schmidt test hammer [1] is a device for measuring the roll hardness using an impacter. It is a modified version of the Schmidt concrete hammer. In this test, a hammer strikes the surface to be measured and the amount of rebound is a measure of the hardness of the roll. It is used widely in European paper mills. The Billy club method is sometimes used by skilled operators who strike the wound roll and can tell by the sound and rebound if the roll has the optimum hardness. The Rho-meter [2] is an instrumented version of the Billy club. A trigger releases the hammer with an accelerometer mounted upon it. As the hammer strikes the rolls the deceleration is measured in units of 'rhos'. A high rho number would infer a hard roll

surface which has caused the hammer to decelerate quickly. The hard roll surface is indicative of a roll with high interlayer pressure.

- 2) Strain: The Cameron test for determining residual strain is a method in which the web layers are sliced using a sharp knife and the layer which was sliced is drawn together as close as possible without introducing any additional tension and the gap is measured [3]. J-lines even though they do not measure strain, can be used to measure the interlayer slippage by measuring the extent of deformation of a mark which has been made on the edge of the web [4]. Strain gages have been used by bonding them to the web to determine the MD (Machine Direction) stress [5]. Strain gages can destroy the web. Once they are placed on the web, the web cannot be used for another experiment. The bonding material, i.e., the glue, increases the Young's modulus of the web locally and hence creates problems. The difficulties involved are covered in the second chapter.
- 3) Interlayer pressure: Pull-tabs have been used as one of the most reliable methods of measuring the pressure in a wound roll [6]. A typical pull-tab is a small strip of steel enveloped in a brass sheet which is placed in the roll during winding. The amount of force required to dislodge the tabs is used to measure the pressure at that point. The Smith roll-tightness tester [7] is a hand-held device which can be used to measure the amount of interlayer pressure by inserting the needle in between adjacent layers of the web. The time taken for the acoustic waves to travel through the layers of a wound roll can also be used to quantify the roll hardness or the radial pressures as a function of radius [8]. FSRs (Force Sensitive Resistor) have been used to measure the radial pressures [9]. The FSRs can be calibrated to determine the pressure at a point in a

roll. Capacitance gages have also been used to measure the radial pressure by placing them in between the layers while winding [10,11].

- 4) Density: The density analyzer can be used to produce pulses and the ratio of the pulses measured by rotary encoders provides a measure of the roll density. Erriksson *et al.* [12] invented the computerized roll-density analyzer.

All measurement methods are accurate but limited in scope. The important requirements are ability to profile along the width and the diameter, accuracy, ability to automatically record data, ease of use, destructive or non-destructive, and cost.

A new technique to determine the roll-structure using strain as the measurement parameter was developed and investigated. This method will be compared with some of the other methods, introduced above, in its ability to meet the requirements, and its limitations.

Chapter 2

LITERATURE REVIEW

This chapter briefly explains some of the widely used roll-structure measurement techniques. The techniques are classified based on the parameter which they measure to determine the roll-structure.

2.1 Impacters

Impacters as the name suggests uses the energy of impact to determine a certain roll's structure. They usually have an independent scale of their own using which a specific impact can be quantified. Measurements can easily be made along the width but not so easily along the diameter provided the machine can be stopped, the roll tested and the machine started again. Recently, Hamad [19] has used a novel way of measuring the coefficient of restitution (C_r) which is defined as the ratio of speed of separation to the speed of approach. He describes an on-line measurement of C_r which is the basic quantity measured by impacters along the diameter. He obtains a set of values for the same along the radius of a roll. Some of the widely used impact tests are described below.

2.1.1 Schmidt Hammer

The Schmidt Hammer consists of a plunger, a spring and a hammer enclosed in a housing which contains a scale and a rider to indicate the maximum movement of the hammer mass in percent of its forward movement. When pressed against a surface, the hammer is released from the calibrated spring and when the hammer is caught on rebound from the surface, the amount of rebound is indicative of the hardness at that point. This instrument measures the rebound height and correlates this to the coefficient of restitution of the impact and hence not in a direct engineering unit.

The hammer is first calibrated against a test anvil and the mean of ten readings is compared with the standard provided. Once the hammer is calibrated, the instrument is used for measuring the roll hardness. However, the accuracy of this device is not quantifiable because it uses its own standard and it also depends on the operator using it. The repeatability of the method again depends on the skill of the operator using it and also whether he uses a definite pattern while measuring. It is shown in fig. 2.1 below.

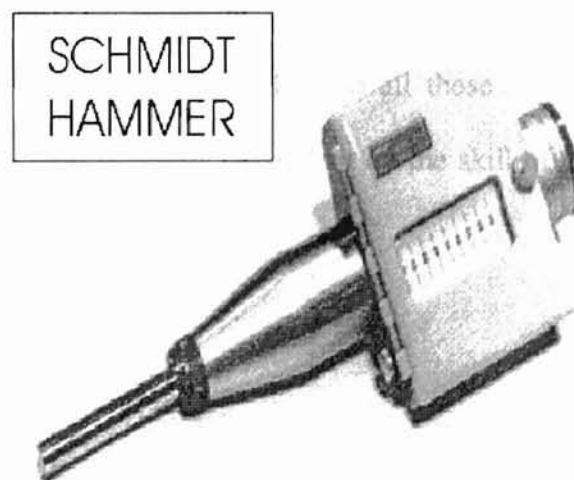


Fig. 2.1 Schmidt Hammer

2.1.2 Rho-Meter

A hardwood Billy club used by a skilled operator enables him to study a roll which has been wound and ready to be shipped. He bases his judgement on the amount of experience he has gained in the industry. When he strikes the club against a roll, the amount of sound produced and the amount of rebound are the quantities he uses to confirm if the roll is wound appropriately or not. He cannot record the results as they are not quantifiable. Also, another skilled operator might not agree with him. The above method can be improved if some sort of sound or vibration sensing device like a microphone or an accelerometer were used. The Rho-Meter idea was conceived from the same principle. The Rho-Meter is very easy to use and it gives a number as its reading depending on the hardness but one which cannot be easily correlated to an engineering unit. When the trigger is released, a plunger hits the roll and the Rho-meter measures the peak deceleration of the hammer striking the roll. This tester is primarily used to check the profile uniformity of hardness across the face of the roll. Care must be taken to check the roll width at equal and small enough increments to get a reliable profile picture. The tester must be held firmly and tangent to the roll circumference. The trigger squeeze must also be uniform as the test progresses. Due to all these limitations, the accuracy and repeatability of the method is highly dependent on the skill of the operator using it. Fig. 2.2 shows the Beloit rho-meter.

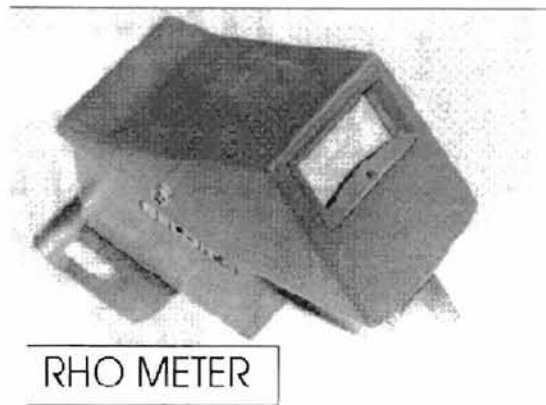


Fig. 2.2 Rho-meter

2.1.3 Paro tester

The paro tester allows one to measure the hardness profile of a roll quickly and accurately. The test is initiated by launching a spring loaded body against the test surface. The impact and rebound velocities are compared resulting in an instantaneous numerical hardness value. The test is portable, easy to implement and extremely accurate. Digital display and inherent data memory help make the parotester as easy to interpret, as it is to operate. Accuracy has been reported of 0.5%.

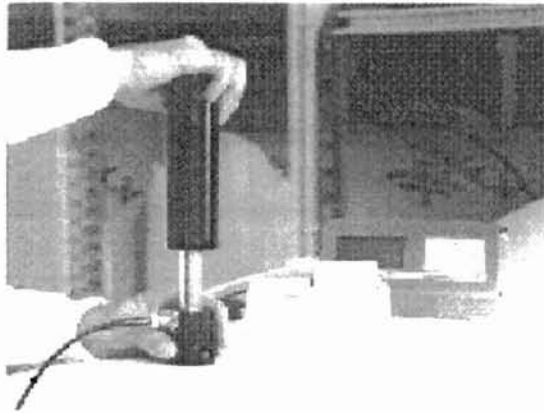


Fig. 2.3 Parotester

2.2 Stress And Strain

Another class of roll-structure measurements is based on web stress or strain. These methods can be used to profile only along the diameter or the MD direction. Using the J-line technique, one can determine the amount of interlayer slippage in a roll as a result of winding or unwinding. Recently, an instantaneous J-line printer was developed in the WHRC by Giachetto [20], which strikes J-lines automatically thus decreasing the number of lines to be struck. For the Cameron test, the roll must be completely slabbed down and destroyed.

2.2.1 Cameron Gap Test

This test is used to measure the residual strain in a roll of paper [3]. This method is mainly used as a qualitative measurement to determine if the strain in a roll to be shipped or stored is within permissible limits or not. The test involves removing the outer layers of the roll and eliminating the layers which have not been in tension or wound

properly. The circumference is then measured. A single layer is cut using a sharp knife and the layer is brought back to its initial position as close as possible without introducing additional tension. The gap is measured. The % residual strain is then calculated as below

$$\frac{\text{Gap Width}}{\text{Circumference of Roll}} \times 100$$

Accuracy in cutting the outer ply and the measurement of the gap are the limitations to this method. This is the most destructive test as the roll is completely destroyed.

The Tappi standard mentions two tests on 40 lb (24 X 36-500) high finish publication paper and it was found that a roll which indicated a 0.25% residual strain snapped off during a press run. Tests on rolls approaching a residual strain of 0.21 – 0.23% should be rejected as substandard for that particular paper. According to Roisum [24], the gap tests tend to be inaccurate for diameters less than about 10” due to the difficulty of measuring the very small gap widths.

2.2.2 J-Line Test

This is a strain-based technique for measuring the magnitude of interlayer slippage as a function of winding or unwinding cycles. Chalk lines or dots from printers are placed on the roll edge when the machine is stopped. After winding, the extent of deformation of the J-line tip is a direct measure of the interlayer slippage. A correlation between the line deformation and runnability can be established.

Giachetto [20], developed an instantaneous J-line printer which allowed him to determine the pressure range in newsprint rolls at which the rolls are extremely soft. The J-line was struck automatically by the printer and could be used to determine the various reasons for tension losses at the outer boundary of the roll. The results of his tests, proved to be useful to study the mechanics of roll winding.

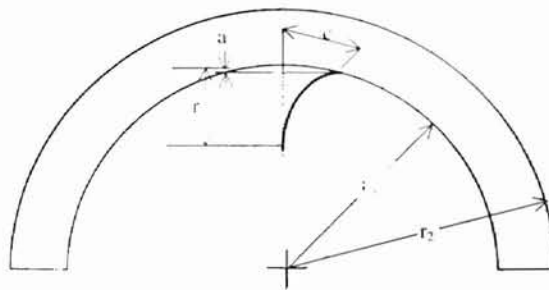


Fig. 2.4 J-line test

The fig. 2.4 shows how the interlayer slippage can be measured using j-lines. The curved line shown in the figure is a J-line. The straight J-line is drawn when the radius of the roll was r_1 and after attaining a radius of r_2 , the extent of deformation of the J-line tip is a measure of the interlayer slippage occurring. c is the maximum circumferential movement, c/a is the slope of tip and r is the depth.

2.2.3 Strain Gages

Strain gages can be bonded to the paper web to measure the stress in the web during the entire process of winding. Circumferential stress was measured with a strain gage glued to the web [5]. The signals were fed through slip rings from the roll to a chart recorder for registration. However, this is a destructive test and also it is cumbersome.

Some of the disadvantages are

- 1) Whatever glue is used, it saturates the paper and stiffens it.
- 2) The strain gage itself results in more than doubling the bending stiffness.
- 3) The strain gage is not at the neutral axis when the web is bent to the contour of the outside of the winding roll. Thus, the gage reads the circumferential membrane strain plus the bending strain.

Hussain, Farrell and Gunning [23] have used strain gages on paper rolls to determine the tension inside a roll. They found that only the outer few layers were in tension and the rest of the roll was in compression. The study was done with three gages consisting of a sandwich of commercial strain gages between two layers of mylar. The investigation of two gages at different radii showed similar results. After about 10 wraps over the gage, the tension drops to zero and additional layers result in greater negative tension until it reaches a asymptotic value. The asymptotic value is higher for higher incoming tension. They report values of -2.5, -3.0 and -3.7 pli. asymptotic tensions for incoming tension values of 1.5, 2.0 and 2.5 pli. respectively.

2.3 Interlayer Pressure

This class involves the measurement of the radial pressure to determine the roll structure. The important methods like the pull-tab and the Smith needle (Smith roll tightness tester) friction testers can only profile along the diameter because the readings are taken along the ends. These types of tests are not very destructive although the Smith

needle while penetrating the layers can damage the edge of a few layers. In all these methods, the pressure inside a roll is determined by using the area of contact of the measuring device with the roll as such.

2.3.1 Pull-Tabs

Pull tabs are strips of steel 12" X 0.5" X 0.001" in dimensions which are enveloped in a brass sheet to maintain a low constant coefficient of friction. The simple arrangement is then inserted into a roll being wound. The pull tabs are then pulled just enough to dislodge them but not completely out of the roll. The amount of force required to pull the tabs, can be used to measure the interlayer pressure in the roll. Pull-tabs relate the interlayer pressure to the amount of force required to dislodge them by using the area of contact and a calibration curve. Pull-tabs have been used by Hartwig [18] for measuring pressures from 10 to 70 psi in newsprint rolls. Beyond this pressure, problems encountered were snapping of the pull-tabs, inability to pull, and the tapes tearing off. He used steel strips which were tempered and polished. The data obtained indicates that there is a high repeatability in the range of 10 to 40 psi with 95% confidence interval values ranging from 0.2 to 2.5 psi. In the 50 to 70 psi range, the 95% confidence intervals range from 3 to 5 psi. for a set of three readings. Hence, the useful range within which pull-tabs are the most useful is 10 to 40 psi. Since the pressures in paper rolls fall in this range, pull-tab is the commonly used measuring method for paper rolls.

Pull-tabs were used to measure the roll hardness by Welp and Schoenmeier[6]. Steel strips of about 3.54 in. long, 0.25 in. wide and 0.002 in thick were inserted into the

roll at regular intervals. They were enclosed in paper sheaths. The force required to pull the strips was used as an indication of the roll hardness. Hakiel [8] used similar pull tabs to measure the radial pressures of a wound roll. Pull tabs made of nylon were used in determining the internal stress of wound rolls of cellophane by Monk [13].

2.3.2 Smith Roll-Tightness Tester (Smith Needle)

The Smith roll tightness tester is a friction-based technique for measuring the radial stress. The Smith roll tightness tester is a device which measures the force required to penetrate a needle to a depth of approximately $\frac{1}{2}$ in. into the face of the rewound roll. The force measured is the sum of the force required to overcome the frictional force between the web and the needle plus the force required to separate the web layers. Since the device is used on the roll face, profiles of the radial pressure as a function of the roll radius can be generated [7]. This method is destructive to light weight grades because the needle might sever a few layers while being penetrated.

The Smith Roll-tightness tester is a small hand-held device and suffers the same drawbacks as the previously explained Rho-meter and the Schmidt hammer tests. This method once again depends on the ability of the operator as to its accuracy and repeatability. Fig. 2.5 shows the smith needle.

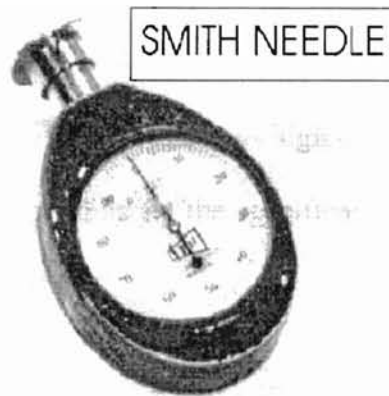


Fig. 2.5 Smith needle

2.3.3 Force Sensing Resistor

The Force Sensing Resistor (FSR) is a device used to measure the load applied by means of a change in its resistance. It is a transducer which comes in two modes; the “Shunt” mode and the “Through-conduction” mode. FSRs have been used for various applications which dictate the accurate measurement of forces such as position sensing, and pressure sensing in wind tunnels [9]. The FSR is made of two polyester sheets sandwiched together. One contains a screen printed pattern of discontinuous conductive fingers and the other, a sensing film consisting of a number of organic and inorganic ingredients suspended in a polymer matrix. The sensing film has very small conductors and semi conductors, ranging from fractions of microns in size. This intimate contact produces a relatively uniform resistance that changes as a function of pressure. FSRs as opposed to the pull-tabs can be used to profile along the diameter and the width but the accuracy along the width is not known [9].

FSRs have been used by Good and Fikes [9], to measure the radial pressure in wound rolls. They were used to measure pressures as high as 150 psi; a pressure at which even the best pull-tab will fail. Depending on the specification on the FSR, they can be used to measure loads as high as 250 psi.

Fikes [21], has used FSRs extensively to conduct tests on Polypropylene rolls. According to Fikes, the calibration of FSRs play a very important role in the determination of the pressures in a roll. Looking at Fikes' data, we can establish the errors in the FSR determined pressures to be 16 psi at a radial pressure of 110 psi and a wound-on-tension of 1110 psi for Polypropylene. FSRs did not yield the expected results the reasons according to Fikes being, possible air entrapment, slippage in the rolls or the tension fluctuations of the winder; the contribution being the most from the latter. Since we did not encounter the latter, or the other problems that Fikes experienced, the useful range of an FSR can be placed in between 200 psi to 400 psi.

2.3.4 Capacitance Gages

Blaedel [10] measured the radial stress in a roll by introducing capacitance gages into the roll while winding. Two brass plates which were separated by paper was used as the capacitor. The capacitance change is a direct measure of the pressure in the roll. Wolfermann and Schroder [11] used an electronic measuring system (EMED), manufactured by NOVEL GmbH, Munchen. The sensor consists of a thin elastic strip of plastic, covered on each side with a thin layer of copper.

2.4 Density

Eriksson, Lydig and Viglund [12] used the density analyzer (fig. 2.6) to measure the density of paper rolls. In the setup, the paper passes the drum (with T_2) and the density is estimated from measurements of the number of revolutions of the drum and the roll. T_1 gives one pulse per revolution and is used to note the number of revolutions of the roll. T_2 gives z pulses for one drum revolution. They developed analytical equations which were based on the number of pulses and hence the revolutions of the roll and the drum; from which they could determine the mean density of the roll. Using the density analyzer, they were able to determine that the wound-off density is lesser than the wound-in density only in the outer layers of a paper roll which was wound four months before the experiment. They determined that factors like rider roll load, web tension, drum torque and web splicing have a direct effect on the density. They were able to demonstrate a close relationship between the radial pressure and the density in a roll. The radial pressure in a roll was measured by using two thin steel blades which were introduced between two layers of a roll. When the grip on the pliers inserting the blades was loosened, a spring forced the blades to separate and the distance gave a measure of the radial pressure at that point.

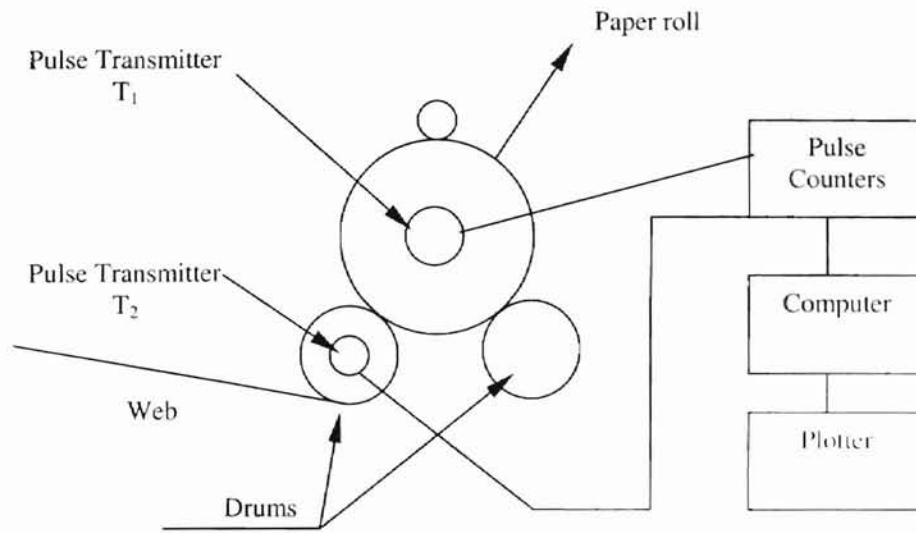


Fig. 2.6 Density Analyzer

Roisum [24], has solved equations for anisotropic and nonlinear anisotropic materials to convert density to wound-in stress provided the original undeformed density, the density during winding, the current radius, the ring radius and material properties such as, moduli and Poisson's ratios are known. He used the model to develop a software for a wound-in stress analyzer. According to him, since the density of a roll decreases with the wound-in stress, the density to stress conversion should not be attempted in the intermediate regions of radius ratios (current radius/ ring radius) but at the extremes i.e. for a 5" current radius, the measurements should be made at a layer count of less than 8 or greater than 26.

2.5 Other Methods

The WIT-WOT winder is a single-drum duplex laboratory winder for measuring the tension wound into a roll as a function of web tension and nip load. Pfeiffer[16] used the winder to measure the tension wound into the web as a function of the nip load and the web tension. The instrument consists of a 40 in. wide winder which can be regulated to run at speed range of 90 to 4000 ft/min, an all-electric control for the nip force, special low-friction cylinders and a fast-responding solid-state tension control. With these arrangements, various families of curves for relating the effect of nip force on wound-in tension at various constant values of web-carrying tension are developed.

The core torque test is a friction-based technique for the measurement of the torque required to cause the core to slip within the wound roll [15]. The torque applied by using a torque wrench yields a single value which is the average of the radial pressure of the roll exerted on the core.

2.6 Theoretical Hakiel Model

The stresses acting on the web are not constant during or after winding. Even after keeping the tension constant, the pressure in the wound web is a function of the radius. Hakiel's [8] model takes into account the non-linear nature of the radial modulus and the orthotropic nature of a roll that is center wound. Hence Hakiel's model is used for all the comparisons of the experimentally obtained strains. The pressures predicted by the Hakiel's model are then verified by measuring the actual pressures in the roll by using pull-tabs or FSRs.

Hakiel's model solves a second order differential equation in radial pressure with two boundary conditions (1) knowledge of the circumferential stress in the outer layer and (2) requiring the deformation of the innermost layer and the outside of the core to be compatible. The two boundary conditions are written in terms of the radial pressure and the differential equation is solved in an accretive fashion. After each solution, the stresses are updated and the state dependent properties are updated. The solution is the radial pressure for the wound roll as a function of radial location. The circumferential stresses can then be determined using the equilibrium equation written in polar coordinates.

The equilibrium equation for plane stress σ in polar coordinates is

$$r(d\sigma_R/dr) + \sigma_R - \sigma_T = 0 \quad (1)$$

The linear orthotropic constitutive equations are

$$\text{For radial direction} \quad \epsilon_R = (1/E_R)\sigma_R - (\nu_{RT}/E_T)\sigma_T \quad (2)$$

and for the tangential direction

$$\epsilon_T = (1/E_T)\sigma_T - (\nu_{TR}/E_R)\sigma_R \quad (3)$$

using Maxwell's relation

$$\nu_{TR}/E_R = \nu_{RT}/E_T$$

and defining

$$\nu \equiv \nu_{RT}$$

and

$$g^2 \equiv E_T / E_R$$

$$\epsilon_R = (1/E_T) - (g^2 \sigma_R - \nu \sigma_T)$$

and

$$\epsilon_T = (1/E_T) (\sigma_T - \nu \sigma_R)$$

using the definition of strain in cylindrical coordinates,

$$r(d\varepsilon_T/dr) + \varepsilon_T - \varepsilon_R = 0 \quad (4)$$

using 1,2,3 and 4, the second order linear differential equation in terms of radial stress can be obtained

$$r^2(d^2\sigma_R/dr^2)+3r(d\sigma_R/dr)-(g^2-1)\sigma_R = 0$$

This equation is solved in an accretive fashion to yield N-1 equations for N laps and using the boundary conditions, we get a set of N+1 equations in N+1 unknowns which can further be solved using the Gaussian elimination to obtain values of δP at each layer.

The radial pressure and circumferential stresses can be used to obtain the circumferential strain using the equation

$$\varepsilon_T = (1/E_T) (\sigma_T - \nu_{RT} \sigma_R) \quad (5)$$

where the subscript T denotes the parameter in the circumferential direction and the subscript R in the radial direction. ε is the strain, σ , the stress and ν_{RT} is the Poisson's ratio

2.7 Summary and Research Objective

Several means of measuring the roll structure have been reviewed. Some were shown to be destructive (Cameron gap). Pull-tabs have been shown to be accurate at low pressures but cannot be successfully applied at high pressures. The Smith needle yields measures of radial pressure but its values are not representative of the entire roll since the

slit edges are always thicker than the nominal web thickness and the needle itself may cause local tearing and thus is destructive. Pressure measurements are preferable in that the pressures can be related easily to roll defects. Methods such as the Rho-meter and the density analyzer have outputs that are difficult to relate to defects. Thus there is a need for a new method that can be used at high pressures with good accuracy and also output measured in engineering units that are relatable to defects. The objective of this research is to study the viability of measuring circumferential strain as a potential roll-structure measurement method.

Chapter 3

EXPERIMENTAL PROCEDURE

A web being wound at a certain web tension, is stretched and in case of low-modulus materials, a considerable strain is exhibited. The web in this strained condition is wound onto the rotating core. When the web is in a stress-free state, tabs (thin strips of sticking tape) are placed on the web at a known distance D_1 . After the web is wound, the distance of separation between the tabs is measured (D_2) and the difference ($D_2 - D_1$) over the original distance D_1 is the experimental strain. The materials that were used for the research were LDPE and a non-woven material (spun polypropylene) [25]. A theoretical model, the Hakiel's model is used which gives pressures in the radial and tangential direction. Using the equation (5) from the chapter on literature review, the theoretical strains are obtained which are then compared with the experimentally obtained strains. To verify the pressures predicted by the Hakiel's model, pull-tabs and FSRs are used. Pull-tabs and FSRs are inserted into the roll being wound at constant intervals and the pressures are determined. Confidence levels are obtained for all the experimental values to account for the errors involved in the input parameters like the web tension, speed, etc. The experimental values obtained during experimentation can be controlled by optimizing the winding tension and regulating it at the prescribed value. At

the same time, care is taken to keep the air entrainment as low as possible because the theoretical Hakiel's model assumes that there is no air entrainment.

The circumferential strain method has been tested with materials which result in high pressures in the wound roll as well as materials with very low internal pressures. Such situations arise in the case of LDPE which can have high internal pressures as high as 200 psi and, in case of a non-woven material where the pressure in the roll can be as low as 5 psi near the core respectively. Also, this method is not costly, it does not require any special skills and it is non-destructive.

3.1 Experimental Procedure

The experiments were accomplished according to the following procedure

1. Theoretical values for the stress and strain were obtained using the Hakiel model. These were obtained by input of measured values of the radial modulus, E_R , tangential modulus E_T , winding tension and other parameters to the Winder software. The inputs to the software are summarized in tables 3.1 and 3.2.
2. Pressure measurements were made to verify the pressures from Hakiel's model using pull-tabs and FSRs.
3. A comparison was made of the theoretical stresses and strains with the experimental stresses and strains and confidence levels were obtained.

3.2 Theoretical Model

To obtain the theoretical Hakiel stresses, Winder 5.0 Beta software was employed. The inputs to the winder software are explained below.

3.2.1 Radial Modulus

According to Hakiel, the radial modulus of the web material was found to be varying as a function of pressure in a wound roll. Hakiel's model takes into account the variation of the radial modulus as a function of pressure. Hakiel [8] assumed that the roll is an orthotropic, elastic cylinder. This cylinder is assumed to have linear properties in the circumferential direction and varying properties in the radial direction. Hence, the Winder program accepts only a radial modulus equation which is a function of pressure and in a cubic form.

The radial modulus equation for 250 gage Low Density Polyethylene (LDPE) was obtained by Qualls [22] as

$$E_R = 167.24 P - 0.09855 P^2 - 0.000422 P^3 \text{ psi.} \quad (6)$$

Since the material used for this research is a 250 gage LDPE, Qualls' equation was used as the input to the Winder software and for all investigations. The radial modulus of a non-woven material was found to be

$$E_R = 4.0834 P + 2.8251 P^2 - 0.3089 P^3 \text{ psi} \quad (7)$$

where, in both equations, P is the pressure inside a wound roll.

3.2.2 Tangential Modulus

The tangential modulus is the elastic modulus measured in the machine direction. During the investigation, the web stresses were not allowed to exceed the plastic limit. To determine the yield stress of the web material, a stretch test was conducted. The stretch test yields load and deformation values using which a stress versus strain graph was plotted and the yield stress was determined based on the 0.2% offset method.

3.2.2.1 Stretch Test

The method consists of preparing a web-length of 50 ft. of the web to be tested (this need not be a constant). The 50 ft. length is taped on one end firmly with a tape with the other end free. The web is allowed to relax before the test is conducted and care is taken to align the web exactly straight which otherwise will affect the readings due to flutter. The web is laid out between two perpendicular marks separated at 50 feet. A clamp with a hook is taped down on the free end. This end is the pulling end. A hand held force gage was used to note the pull-force applied and the resulting strain was calculated and plotted. The stretch test proved to be a tricky one. The force had to be applied constantly and in the event of releasing the force while stretching, there was a noticeable decrease in the load necessary to maintain the stretch due to the visco-elastic nature of the web. It was found that a 50 ft. length of LDPE was easily stretchable to 30 ft., after the 50 ft. mark, denoting the extremely ductile nature of the web. But the force required to pull it to 30 ft. was not high (approximately 30 lb.). After a stretch of approximately 34 ft.

beyond the 50 ft. mark, the web broke resulting in a ductile fracture. The site at which the ductile fracture occurred, showed severe plastic deformation similar to the necking in a tension test specimen.

This test was conducted in this fashion because there was great difficulty reported in performing the conventional ASTM standard methods to determine the elastic properties of the web material. The problems reported were grip slippage and specimen misalignment problems. Also the errors were non-repeatable. The web is pulled slowly and continuously. Continuity is necessary because due to the visco-elastic nature, the web starts relaxing and the force starts decreasing. Readings are taken of the amount of deformation. A stress vs. strain plot is then obtained using the load and deformation. Three such tests were conducted and the yield strength of the web was found to be 800 psi. Hence all loading were restricted to below this level. Fig. 3.1 is the plot obtained.

Eventhough from the stress-strain fig. 3.1 we can get 21,000 psi as the tangential modulus, the tangential modulus of the 250 gage LDPE web was found to be 24,000 psi by Qualls [22] and was used for all experiments because he measured it below the glass transitions temperature of LDPE. This was one of the important parameters to be input into the Winder software. Similarly, conducting the stretch test on a non-woven material resulted in a tangential modulus of 8000 psi.

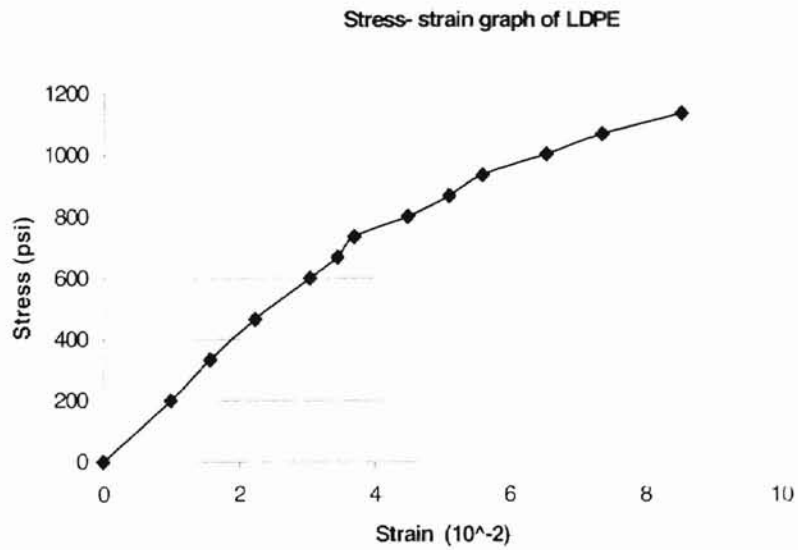


Fig. 3.1 Stress Vs Strain plot for LDPE obtained by stretch test

The inputs to the Hakiel model using the Winder software gives the tangential stress σ_T , and the radial pressure σ_R . The tangential modulus, E_T is already known by the stretch tests. The strain, ϵ_T in the tangential direction is

$$\epsilon_T = (1/E_T)\sigma_T - (v_{TR}/E_R)\sigma_R \quad (8)$$

This strain ϵ_T , is compared with the strain obtained using the circumferential strain method.

Description	Value
Web tension	100 psi and 200 psi
Radial Modulus	$E_R = 167.24 P - 0.09855 P^2 - 0.000422 P^3$ psi.
Tangential Modulus	$E_T = 24000$ psi
Poisson's ratio, ν	0.01
Thickness of web	0.0025 in.
Width of web	6 in.
Core: Carbon steel	30,000,000 psi
Core Internal Diameter	1.492 in.
Core Outer Diameter	1.69 in.
Wound roll OD	(5.0 ± 1.0) in.

Table 3.1 Inputs to the Winder software for LDPE

From equation (8), it is evident that the most important parameters are the radial and tangential moduli. The coefficients of the E_R and the E_T have to be in the format mentioned in table 3.1 since they depend on the pressure in the roll to different degrees. The thickness of the web is constant over the width of the web. The core internal diameter and the external diameter are required to take the radius measurements and they have to be accurate to the second decimal. The winder software is most sensitive to errors in the winding tension and less sensitive to errors in E_R and E_T .

Description	Value
Web tension	71.89 psi.
Radial Modulus	$E_R = 4.0834 P + 2.8251 P^2 - 0.3089 P^3$ psi
Tangential Modulus	$E_T = 8000$ psi
Poisson's ratio, ν	0.01
Thickness of web	0.005 in.
Width of web	4.173 in.
Core: Carbon steel	30,000,000 psi
Core Internal Diameter	1.492 in.
Core Outer Diameter	1.69 in.
Wound roll OD	(5.0 ± 1.0) in.

Table 3.2 Inputs to the Winder software for Non-woven

Fig. 3.2 is an error plot which takes the worst combinations of the two moduli and shows how much the strain can vary. For this analysis on a non-woven web, the web tension as 71.89 psi, radius as 5.0 in. and the speed as 25 fpm were kept constant. The E_R and the E_T were varied keeping one of them a constant. The average of the nine readings were used to calculate the strains and plotted. The three E_R values obtained during the E_R tests were

- I. $-0.2978 P^3 + 2.8412 P^2 + 3.5601 P$
- II. $-0.2932 P^3 + 2.6418 P^2 + 4.5234 P$
- III. $-0.3357 P^3 + 2.9924 P^2 + 4.1669 P$

The E_T values were allowed to vary ± 2000 psi from the value which was used for all experiments i.e. 8000 psi because according to Qualls [22], the standard deviation of the E_T values for LDPE was 2644.

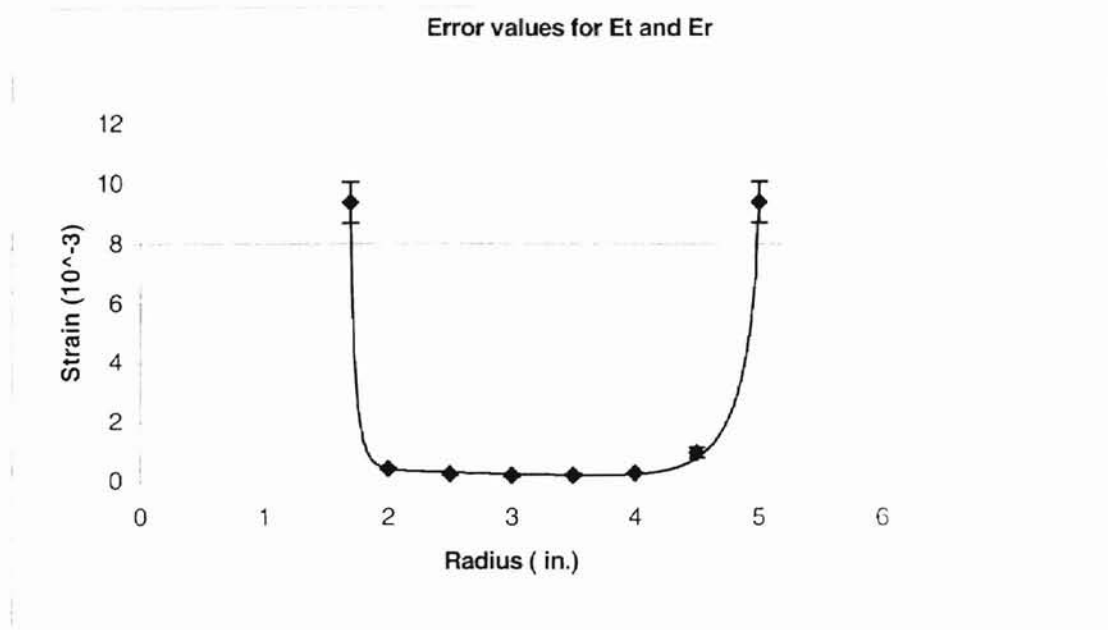


Fig. 3.2 Maximum possible variation in strain due to E_R and E_T

The effect of the errors in the modulus values for small tangential strains is less when compared to higher strains, where, the effect is pronounced. Hence, care must be taken while measuring the E_R and E_T values. In a material which results a large strain, these can be critical.

3.3 Pressure Measurement

Pressure measurements of a wound roll were taken to verify the stresses given by the Hakiel model. The techniques adopted to obtain the experimental pressure measurements were the pull-tab and the FSR. An FSR before being used, had to be

calibrated for LDPE web. Pull-tabs have long since been used in WHRC and the repeatability and accuracy of pull-tabs is better than FSRs. Hence both the techniques were used to determine the experimental pressures in a wound roll.

3.3.1 Calibration Of FSR

The FSR changes its resistance based on the load acting upon it. To measure the radial stress in the wound roll, the FSRs were calibrated using the INSTRON and a stack of web to obtain a pressure versus resistance plot.

3.3.1.1 Loading Routine

The loading sequence of the FSR has a considerable effect on the resistance values obtained. In the work done by Good and Fikes [9], they explain two modes of loading - uploading and downloading. Uploading involves the loading of the FSR in a fashion in which the load never decreases. The FSR was placed within a stack of web (6 in. x 6 in. x 1 in.) such that the load sensor is in the middle of the stack. 100 psi load was applied which was the lowest limit of our calibration sequence and the FSR was maintained at that load for a maximum duration of 30 min. The FSR was then loaded in successive incremental steps to a maximum of 700 psi without removing the FSR. Resistance measurements were taken at each load. Each load – resistance value pair was taken for three different FSRs and each FSR was subjected to the sequence three times. The average of the nine readings was then calculated and tabulated. The curve that was obtained, was used as the master curve for the actual experiments.

In downloading, the FSR is loaded to the maximum limit and then the load is decreased in successive steps at some point in the sequence. The uploading sequence is practical for a material like newsprint because of the constant tension involved in the center winding. But, in the case of visco-elastic materials like LDPE, the stress in the roll after being wound is not constant. The web tries to relax from its tensioned state to a state of equilibrium. This condition is similar to a downloading sequence as explained above. But, if the stress measurements are taken immediately after the web is wound, the web would not have started relaxing yet, and the uploading sequence can be approximated to the stress state. This approximation is necessary because there has been no record about how much the web relaxes and how long it relaxes [9]. Fig. 3.3 shows an uploading sequence.

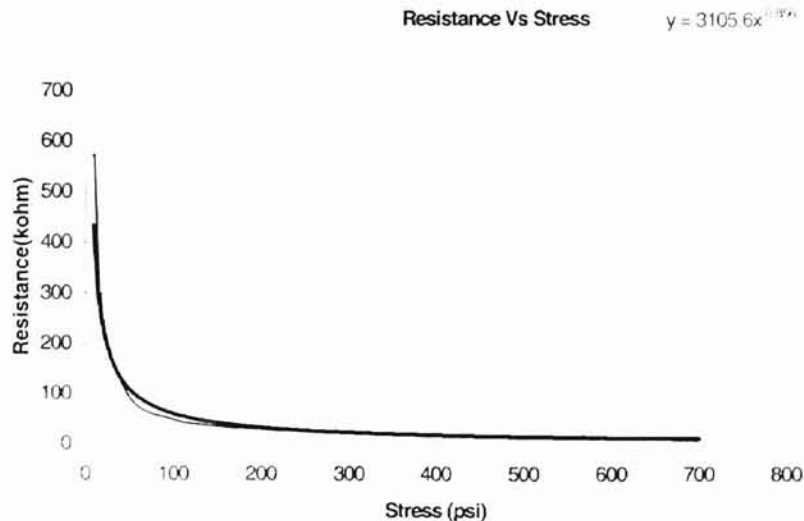


Fig 3.3 Calibration of FSR (uploading)

After all pressure measurements were done using the FSR, they were recalibrated to find out how considerable the calibration had changed if it had. It was noticed that there was a negligible change in the coefficients of the equation obtained during the first calibration. It was concluded that the calibration does not get affected much by using the FSR for pressure measurements where it can be subjected to high pressures for a long time.

3.3.2 Calibration Of Pull-Tabs

A stack of the web similar to the one used for calibration of the FSRs was prepared (6 in. X 6 in. X 1 in.) and loaded with the pull tabs in the middle of the stack. A similar unloading sequence was adopted for calibrating pull-tabs and the pressure versus pull force graph was obtained as shown in fig. 3.4. Three different pull tabs were pulled at the same pressures and for three trials for each tab. The average of the nine readings were plotted and the equation which resulted was used for the radial pressure measurements. Pull-tabs were used to confirm the pressures predicted by Hakiel's model when pressures were low.

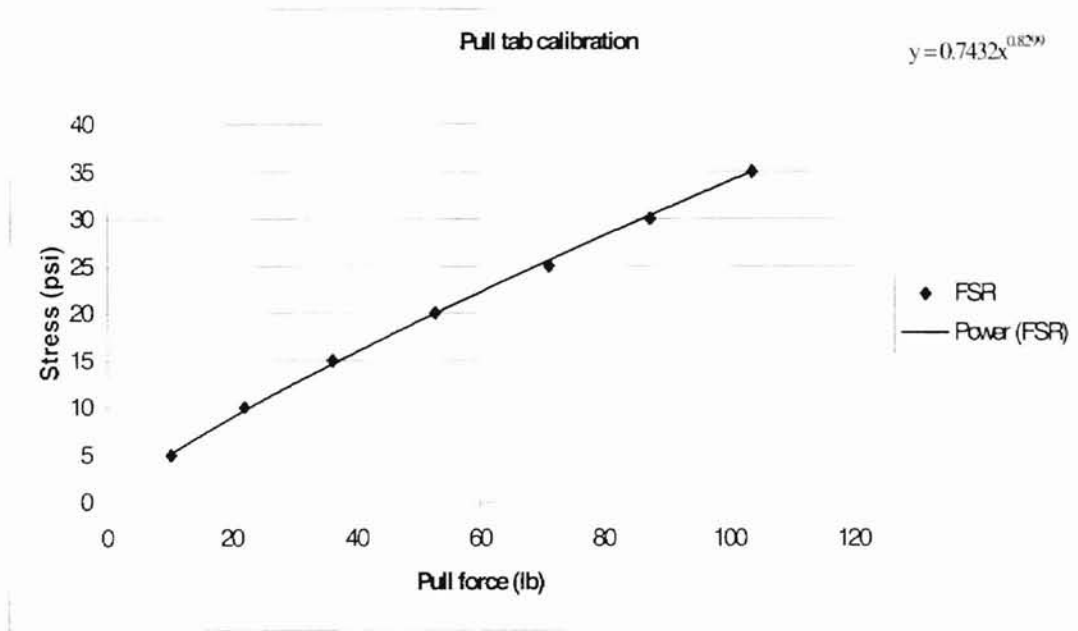


Fig 3.4 Pull-tab calibration (uploading)

3.4 Winding

LDPE was the material used since lot of research had been done already on the material by Qualls [22]. In the early stages of research, an LDPE web of 1 mil (0.001 in.) thickness was chosen. The loads applied resulted in wrinkles and made the web unusable for further tests. The web would wrinkle with even slight lateral motions. Hence, a 2.5 mil (250 gage) LDPE web was used subsequently. The properties of LDPE 250 gage were established by Qualls [22]. The advantages were that the winder could be run at higher web tensions than for a 1 mil web and higher tensions can be maintained fairly constant. A diagram of the winder and the configuration used to wind the web is shown in Fig 3.5. In this study, the focus was on center winding and as such, the nip roller was retracted from the winding roll and was bypassed.

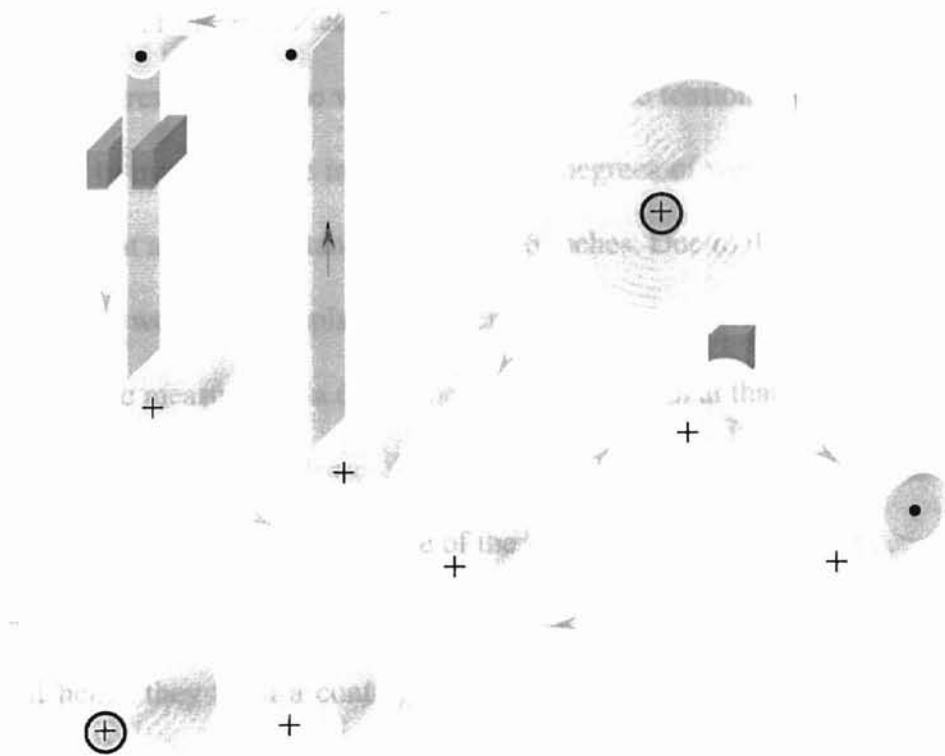


Fig. 3.5 Experimental set up

Legends :

- | | |
|--|--------------------|
| 1. Unwind Station | 6. Nip Roller |
| 2. Web lateral motion guide | 7. Winding Station |
| 3. Infra red sensor for lateral motion guide | |
| 4. Web line tension feedback roller | |
| 5. Speed Comparator | |

3.5 Experimental Procedure

A modification of the J-line technique [7,4] was at first thought as the technique to measure the strains resulting in the web due to the web line tension and other winding parameters. Instead of using a single ink jet every 360 degrees of web rotation [20], two dots would be placed at a known distance apart, say, 6 inches. Due to the tangential strain of the web, the dots would be displaced further apart by a very small amount. The variation, which can be measured, is a direct measure of the strain at that point.

This method was however abandoned because of the following reasons:

1. In the case of the J-line technique, the dots are placed at every 360-degree rotation of the web and hence they form a continuous line along the side which can easily be observed. However, in this case, two dots are placed at every one-half inch increment of the radius of the web from the core. The dots would not be visible among 2000 layers of web with the naked eye and higher resolution techniques, like microscopes have to be used to observe the dots.
2. The web even though aligned using a infra-red alignment device will not attain a perfect winding without some minute telescoping. This will not allow the dots to be clearly seen even with the help of high resolution devices.
3. Ink will not stick to the surface of non-permeable materials especially LDPE.

3.5.1 Tabs

A new mode of indicating distances on the web had to be contrived and the concept of placing a more conspicuous object, which will overcome all the above obstacles, was conceived. A bar of aluminum was machined with two 0.5 in. slots which could hold two strips of any material at exactly 5.998 (~ 6) in. apart. Steel strips of 0.001 in. thickness and ½ “ wide were cut to approximately 2 inch length and were taped down to the edge of the web using the machined bar of aluminum. The web was stopped in between winding and the steel tabs were placed on the aluminum bar such that about an inch was protruding outside with tapes stuck to them. The machine was stopped while placing tabs because of the following reasons:

1. The tabs couldn't be placed firmly on a moving web.
2. The web is stretched and is in tension while running. Any tabs placed, will be placed on a pre-tensioned web. For easier, and accurate, measurement of strains, the web was stopped, and when it is ensured that the web is completely relaxed, the tabs were placed.

Care was taken to make sure that the edge of the web was aligned to the edge of the aluminum bar and the tabs were taped down to the web. The web so prepared was then allowed to wind without any sort of restrictions on the tension or speed because the stopping and starting of the web results in telescoping which will not give out a true wound roll. The web was finally wound at the testing tension and speed. Steel tabs were used because they could be used readily without any modifications. Modifications in the

previously used materials (like brown tape and cellophane) were trimming of the edges such that the edges are perpendicular to each other. Since steel tabs were appropriate for the job, in the as received condition, they could be used as they were. Approximately 2 in. lengths of the tabs were cut and they were stuck carefully to the web. The results were unsatisfactory and unreliable. This led to the abandonment of steel as tab material and led to the search of a material for the tabs which had properties similar to those of the web being wound.

Audio cassette tape was proposed as another material. But since the device to measure the strain, i.e. vernier is not very accurate, it was also discarded because they were rather flimsy. Also, the cassette tape tabs were very thin and they would be subjected to a lot of twisting due to the pressures in the wound roll.

Sticking tape tabs of $\frac{1}{2}$ " width were used as their frictional properties matched almost to the properties of the web. Also, they were in a pre-finished state. The tabs henceforth shall be referred to as Shim tabs. There was a certain level of conformity among the strains obtained by using the tape tabs. Hence it was decided that these tabs were to be used for all experiments. Fig 3.6 shows how the tabs look after they are placed in the roll. They are placed on a roll with a radius of 5.4 in. The tabs are placed such that approximately $\frac{1}{2}$ " will be sticking out to make the measurements.

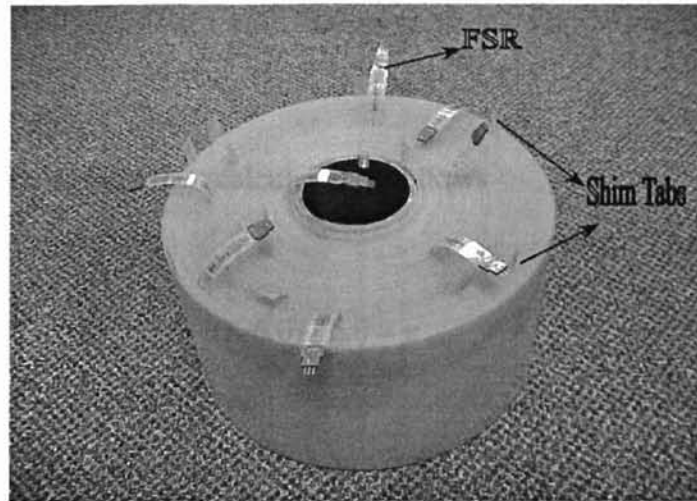


Fig. 3.6 Shim tabs and FSRs

3.6 Strain Measurement

The procedure to measure the experimental strains is described in this section. The straight-line distance is the distance between the tabs and was measured using a vernier calipers. Using the radius value R (again measured by a vernier), at which the tab is placed, and the arc-sine formula, the arc-distance between the tabs is calculated. If L is the straight-line distance between the tabs, and R is the radius at which the tabs are placed, the arc-sine formula gives,

$$\sin^{-1} ((L/2)/R) = \theta / 2 \quad (9)$$

from which, θ , the angle of separation between the tabs is calculated. The arc-length between the tabs is then obtained by the arc-length formula

$$S = R \theta$$

The experimental strains are then calculated as follows

$$(S-6.0) / 6.0 = \epsilon_{\text{expt}} \quad (10)$$

Or

$$(2 \sin^{-1}((L/2)/R) \cdot R - 6.0) / 6.0 = \epsilon_{\text{expt}} \quad (11)$$

The strains obtained experimentally (using the arc-length formula) and theoretically (using Hakiel stresses) are plotted to get a comparison and hence to prove Hakiel model experimentally using strains as the means of comparison.

3.7 Resolution and Limitations

The circumferential strain method has its limitations. The method uses a vernier-caliper which has a least count of 0.001 in. Hence, readings can be accurate only to the third decimal which are easily encountered during strain measurements. But, due to the involvement of radius as a crucial parameter required for the strain, the accuracy is affected further if radius measurements are not taken correctly. From table 4.2 it can be seen that strain values of 0.0009 were measured using the method. But, this strain value was obtained using LDPE which has a modulus of 24 ksi. In industry, such as the paper & pulp, the material used commonly is newsprint which has a modulus of 700 ksi. Such high modulus material will demonstrate a strain which will be far less than the strains in

LDPE. The method must be modified by placing tabs further apart for such measurements.

Newsprint and LDPE having the same thickness have varying properties. In newsprint [18] with a web tension of 6 lb. or 350 psi, the pressures inside the roll was below 50 psi. Pull-tabs can be used to measure pressures in the range of 0 to 60 psi. Pressure measurements were conducted on newsprint with pull-tabs. In LDPE, with a 100 psi. web tension, the radial pressure reached 90 psi near the core. With such high pressures, it is not possible to use pull-tabs for measurements. FSRs are used in this case to measure the pressures. Pull-tabs even when used were not used in the regions where the pressures exceeded 50 psi. The point is, the circumferential method uses an external measurement which is a clear portrayal of the roll's internal data and hence is a useful method. It can be used to determine the roll-structure even when the wound roll has very high internal pressures. The experimental values obtained can be readily compared to the theoretical model and hence can be validated. The Cameron gap test cannot be used on a visco-elastic material like LDPE because as soon as the layer is cut, the web would start relaxing and hence measurements would be erroneous.

3.8 Resolution Obtained

In the measurements the most difficult part was measuring the straight line distance. The radius measurement was accurate. This straight line distance is further approximated by the arc-sine formula and the errors of the calculating device. Hence,

taking into consideration all these errors, the resulting value can be approximate only to 0.001 in.

To demonstrate the errors involved and hence the resolution of the method, a typical measurement will be made with errors in length, radius and finally in both the values. Each value will be decremented by 0.001 in. which is the least count of the measuring device and using the value and the formula, the strain will be calculated. Consider a hypothetical straight line distance between the tabs to be 5.0 in. and the radius to be 3 in. The strain calculated using the formula (11) will be

$$\begin{aligned}\epsilon_{\text{expt.}} &= (2 \sin^{-1}((L/2)/R) \cdot R - 6.0) / 6.0 \\ &= (2 \sin^{-1}((5/2)/3) \cdot 3 - 6.0) / 6.0 \\ &= 0.01488\end{aligned}$$

Description	Value	Strain	% Error
Radius	2.999	0.0147	1.2
Length	4.999	0.0151	1.5
Both	2.999, 4.999	0.015	0.8

Table 3.3 Resolution of the method

The results in table 3.3 show that the errors involved in measuring the strains is not very high assuming that the 0.001 in. error is the maximum error that can be induced.

Chapter 4

RESULTS

This chapter deals with the results obtained using the circumferential strain method. The strains measured using the techniques discussed in the previous chapter are compared with the Hakiel generated strains and plotted. The results obtained in this chapter were the average of three winds and 95% confidence intervals for a population of three values are established. The individual data points are shown in the appendix.

4.1 LDPE Wound At 100 psi Tension

The shim tabs were placed at regular radius intervals into the web while the web was being wound. Since this is a non-destructive test, the roll was wound, the strain values measured, and the roll wound again. The web was wound three times and strains measured each time. The average of the three strains was calculated and the errors involved, noted. The experimental results consistently follow the theoretical model. The comparison graph, Fig. 4.1 and table 4.2 exhibit the correlation between the theoretical (Hakiel) strains and the experimental strains. They show a good correlation at all regions except near the core where the following problems were encountered during winding and testing

- 1) Near the core, the winding parameters were not consistent with the rest of the roll. The initial few layers could not be wound at the same tension as the rest of the roll because it took some time for the magnetic brake controller to achieve the desired tension.
- 2) The error contributed by the vernier increases as measurements are taken closer to the core. Assuming that the vernier gives an error of 0.001 in. for every measurement done, and that the radius was measured precisely, Table 4.1 shows how the experimental strain is affected at different radii. To perform this test, a set of values from a winding trial of LDPE was chosen and the measured straight line distances were incremented by 0.001 in. with the measured radii unchanged. We can see that an increase of 0.001 in. in the straight line distance values results in an appreciable variation in the strain value measured near the core than at the outer radius. This might be one of the contributing factors to the especially high strains near the core.

Radius (in.)	Actual Strains (10^{-3})	Modified Strains (10^{-3})	% Change
2.152	2.293	3.259	42.13
3.328	0.929	1.197	28.85
3.792	1.188	1.426	20.03
4.487	2.063	2.276	10.32
5.028	3.302	3.503	6.09
5.308	3.567	3.765	5.55

Table 4.1 Error in measurements by vernier near the core

The following sections show the experimental strains that were obtained and which are compared to the theoretical strains given by the Hakiel's model. The web tension was 100 psi and the winding speed was 22 ft/min.

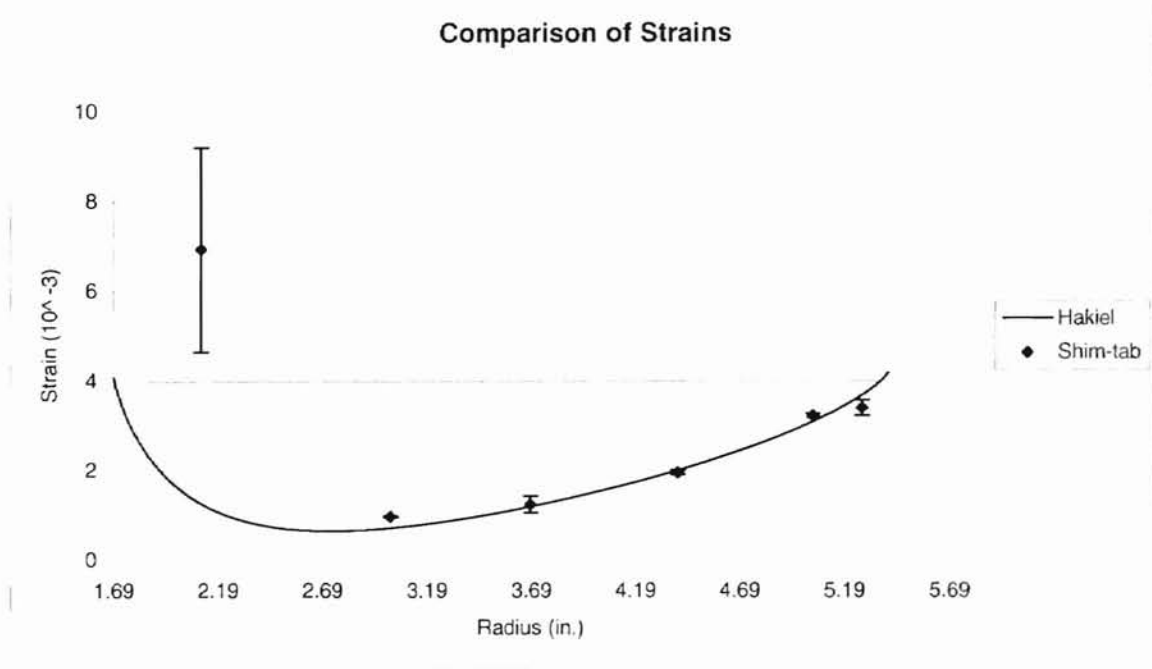


Fig. 4.1 Comparison of strains (LDPE, 100 psi)

Radius	Strains (10^{-3})			Average	Std. Dev	Confidence 95%	Error \pm
	1	2	3				
2.108	2.292	9.077	9.393	6.921	4.012	4.540	2.270
3.013	0.928	0.975	0.984	0.962	0.030	0.034	0.017
3.687	1.188	0.943	1.605	1.245	0.335	0.379	0.189
4.395	2.063	1.904	1.891	1.953	0.096	0.108	0.054
5.04	3.301	3.211	3.155	3.222	0.074	0.083	0.042
5.275	3.267	3.166	3.73	3.388	0.301	0.340	0.170

Table 4.2 Error analysis of strains (LDPE, 100 Psi)

The table 4.2 shows the three trials of experimental strains and the 95% confidence levels calculated on the data. Except for the readings near the core, the rest of the values demonstrate a good equivalence with the theoretical curve.

In order to determine the strain confidence intervals in terms of pressure, a typical value of strain from table 4.2 at a radius of 3.687 in. was chosen since it was one of the worst cases of confidence intervals encountered. The web tension was varied using the winder software to yield radial pressure values that results in the confidence interval of the strain value chosen. It was found that the pressure variation was 4 psi. Now, this can be compared to Fikes' [21] results for measurement of radial pressure using FSRs.

4.2 Pressure Comparison Using Pull-Tabs

Three pulls using pull-tabs were performed on a wound web, averaged, and the pull-tab stresses obtained using the calibration curve were compared with the theoretical Hakiel stresses. The comparison between Hakiel pressures and the pull-tab pressures is shown in fig. 4.2 along with the error analysis in table 4.3. Good correlation was found between the theoretical and the experimental stresses. They were also found to be consistent. Three rolls were wound with the pull-tabs in the same radial location. The core pressure far exceeded the range of pull-tabs and so, pull-tabs were not placed near the core.

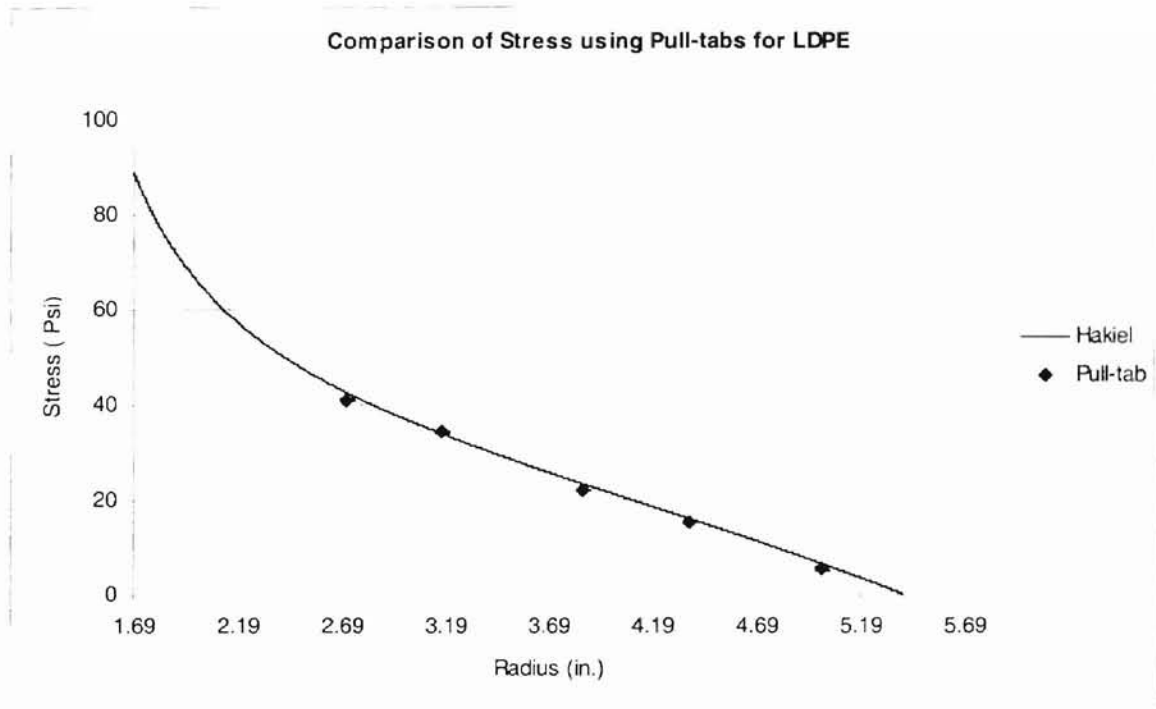


Fig. 4.2 Comparison of stresses using pull-tabs (LDPE, 100 psi)

Radius	Pull-tab stress (Psi)			Average	Std. Dev	Confidence	Error ±
	1	2	3				
						95%	
2.714	40.86	41.14	41.04	41.013	0.142	0.161	0.080
3.167	34.36	34.44	34.15	34.317	0.150	0.169	0.085
3.859	21.9	22.16	22.13	22.063	0.142	0.161	0.080
4.369	15.35	15.35	15.4	15.367	0.029	0.033	0.016
5.139	6.4	5.3	4.92	5.540	0.769	0.870	0.435

Table 4.3 Error analysis of pressures using pull-tabs (LDPE, 100 psi)

4.3 Pressure Comparison Using FSR

The theoretical and the experimental stresses were also compared using Force Sensitive Resistors. As explained above, since the core pressures were too high for pull-tabs to measure, they were made using FSRs. FSRs were inserted into the roll while it was being wound and the resistances were measured using a multi-meter.

From fig. 4.3 and the error analysis shown in table 4.4, it can be seen that the results are not as good as the pull-tab results; further asserting the fact that roll-structure measurement using pull-tabs is a very reliable technique.

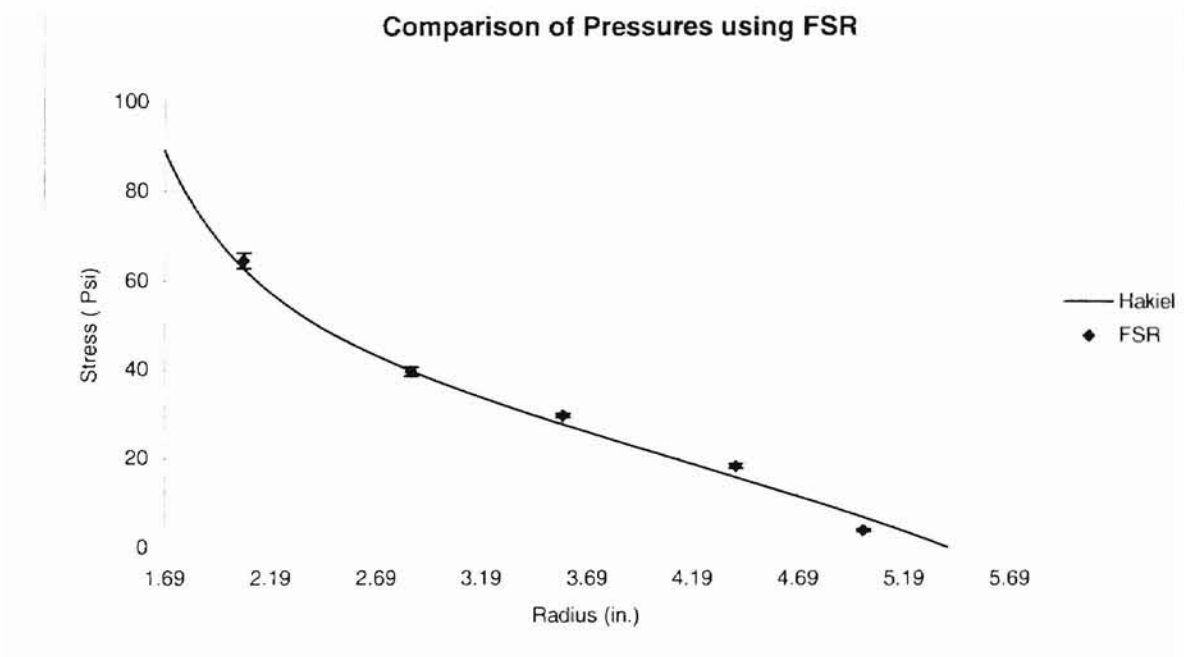


Fig. 4.3 Comparison of stresses using FSR (LDPE, 100 psi)

Radius	FSR stress (Psi)			Average	Std. Dev	Confidence 95%	Error ±
	1	2	3				
2.059	66.65	60.87	65.75	64.423	3.110	3.519	1.760
2.852	41.22	37.72	39.55	39.497	1.751	1.981	0.990
3.577	30.08	28.66	29.89	29.543	0.771	0.872	0.436
4.398	17.17	18.5	18.88	18.183	0.898	1.016	0.508
5.2	3.85	4.35	3.2	3.800	0.577	0.653	0.326

Table 4.4 Error analysis of pressures using FSRs (LDPE, 100 psi)

4.4 LDPE Wound At 200 psi Tension

The circumferential strain method was verified at a higher web line tension of 200 psi. The comparison of strains is shown in fig. 4.4 along with the error analysis in table 4.5.

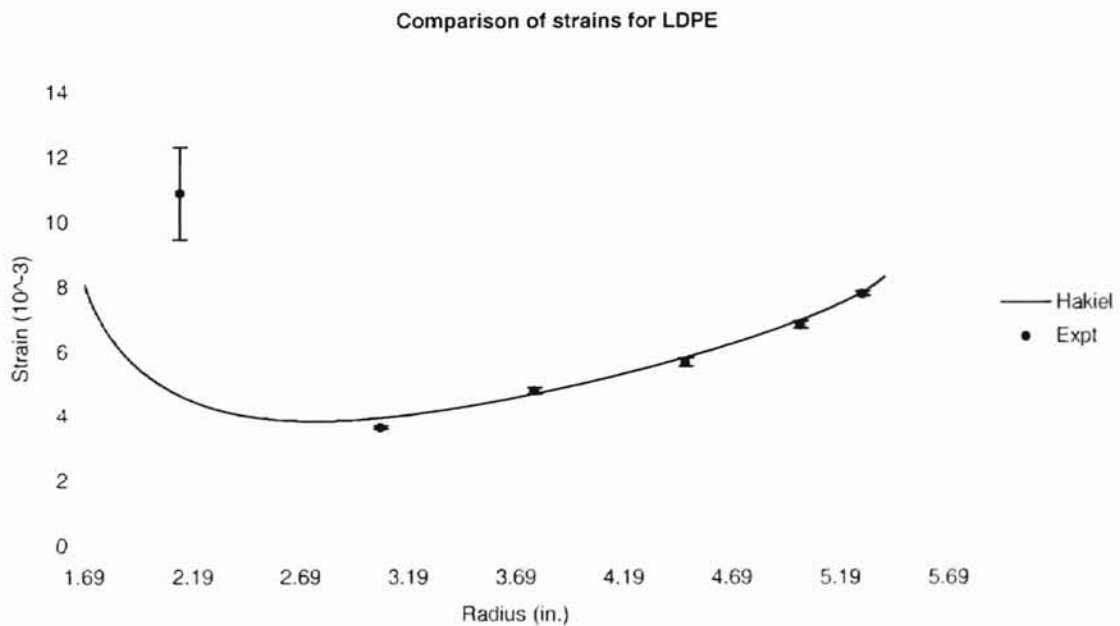


Fig. 4.4 Comparison of strains (LDPE, 200 psi)

Radius	Strain (10^{-3})			Average	Std dev	Confidence	Error \pm
	1	2	3				
2.127	8.063	12.722	11.928	10.904	2.492	95% 2.820	1.410
3.06	3.689	3.725	3.575	3.663	0.078	0.089	0.044
3.776	4.701	5.004	4.678	4.794	0.182	0.206	0.103
4.475	5.409	5.758	5.878	5.682	0.244	0.276	0.138
5.007	6.925	6.609	6.982	6.839	0.201	0.227	0.114
5.291	7.902	7.831	7.649	7.794	0.130	0.148	0.074

Table 4.5 Error analysis of strains (LDPE, 200 psi)

4.5 Pressure Comparison Using FSR at 200 psi Web Tension

A pressure comparison of the Hakiel stresses was made using FSRs. Since the pressures in the wound roll were very high (as high as 276 psi at the core), pull-tabs could not be used. Also, the results using FSRs were not as accurate as the 100 psi case. The maximum pressure that could be measured by these FSRs was 225 psi. 95% confidence intervals are obtained for a set of three readings and shown in fig. 4.5 and table 4.6. The individual set of readings are shown in the appendix.

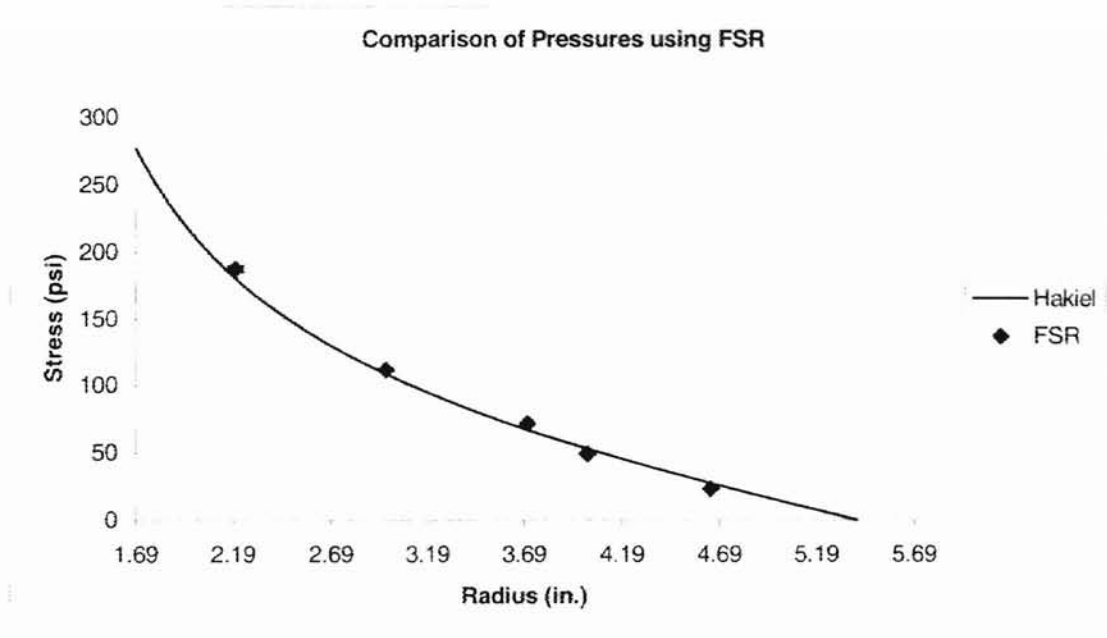


Fig. 4.5 Comparison of pressures using FSRs (LDPE, 200 psi)

Radius (in.)	Stresses (Psi)			Average	Std.dev	Confidence 95%	Error \pm
	1	2	3				
2.20	190.40	189.20	183.10	187.57	3.91	4.43	2.21
2.98	112.60	112.40	110.20	111.73	1.33	1.51	0.75
3.71	71.90	70.20	72.60	71.57	1.23	1.40	0.70
4.01	48.70	47.90	50.90	49.17	1.55	1.76	0.88
4.65	22.90	23.50	22.60	23.00	0.46	0.52	0.26

Table 4.6 Error analysis of pressures using FSRs (LDPE, 200 psi)

4.6 Non-Woven Material

The results reviewed so far were for LDPE. The same experiments were conducted on a non-woven material to confirm the circumferential strain method. This was a material with a very low Young's modulus of 8000 psi. The results were satisfactory with this material at all regions except the core due to unreliable winding.

Similar to LDPE, all the comparison tests were conducted on this material. It was noticed that the pressures inside the wound roll were very small when compared to those of LDPE. The pull-tab method of pressure measurement was adopted as FSR resistances were very high for small pressures and large variations were noted even at constant loads. The pull-tab calibration curve is shown below.

4.7 Pull-Tab Calibration For Non-woven Material

As seen from fig. 4.6, the pull-force needed to pull the tabs increases linearly as the pressure inside the roll increases. Three different pull-tabs were pulled in three trials, one for each pull-tab. Each pull-tab at a particular load was pulled three times to minimize the errors involved in pulling the pull-tabs.

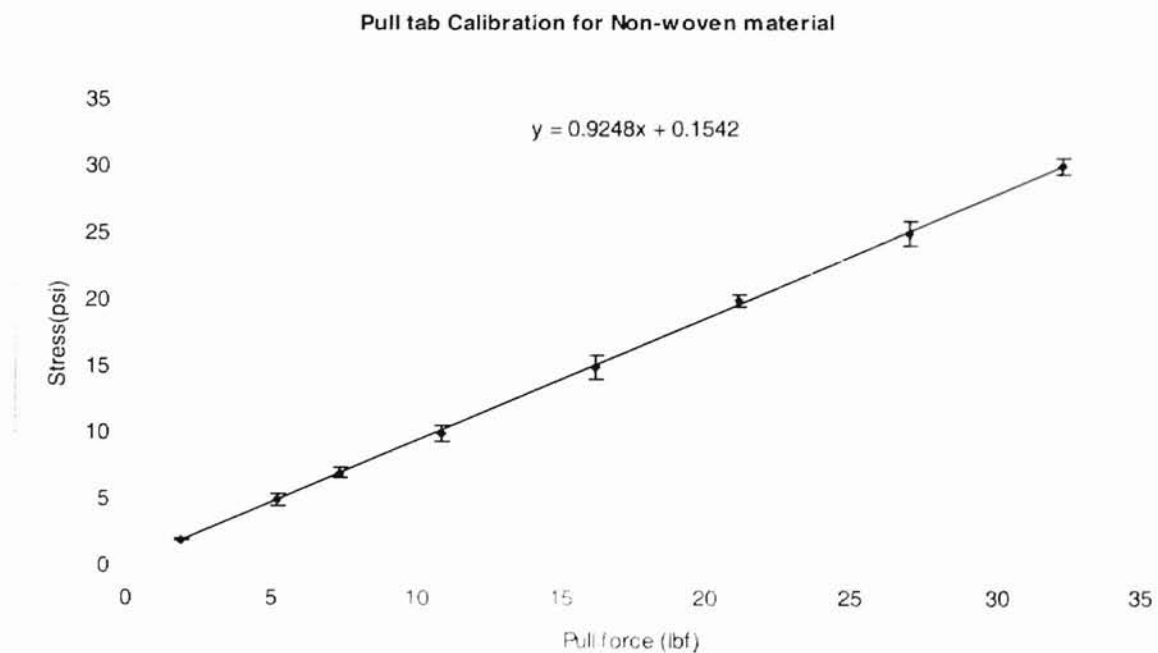


Fig. 4.6 Pull-tab calibration for non-woven material

4.8 Pressure Comparison For Non-woven Material

As explained for LDPE, a pressure comparison was made even for the non-woven material. Three winds were done and the results averaged. Each of the pull-tab reading in the table below is the average of three pulls on a single pull-tab during a single wind. This comparison is shown below. Even in this material, due to the unreliable windings at the core, the pressure measurement could not be made well near the core. As seen in fig. 4.7, the pressure rapidly decreases from the core, remains constant and decreases gradually. The error comparison is shown in table 4.7.

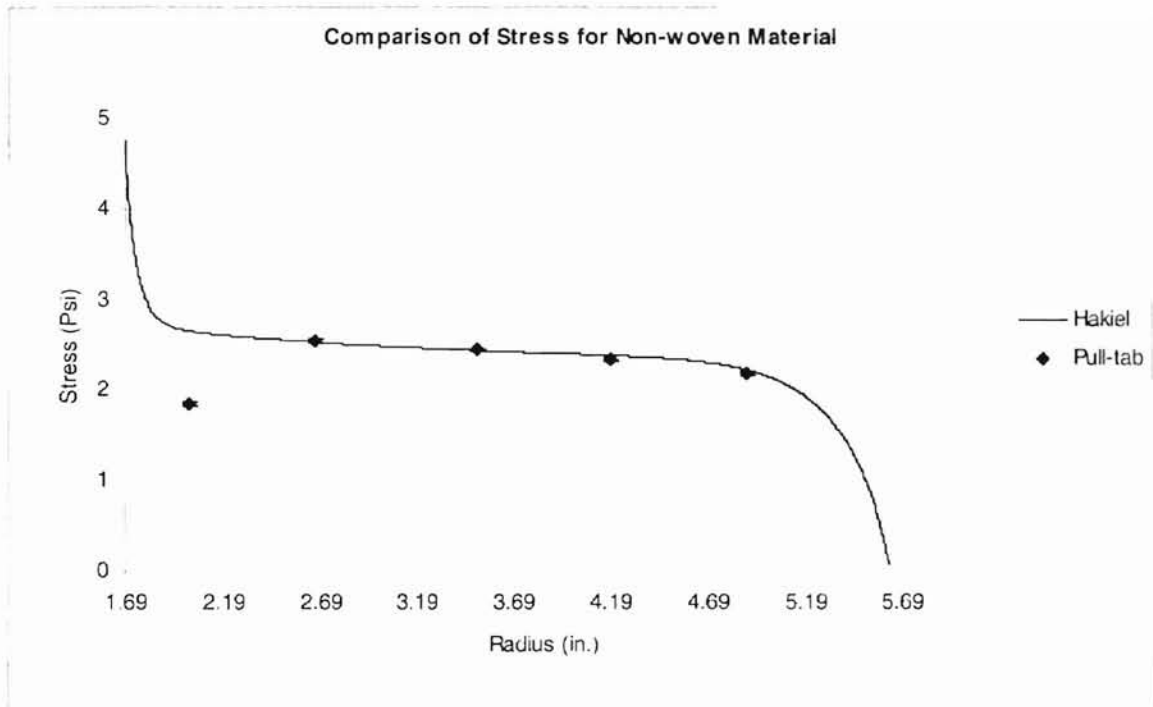


Fig. 4.7 Comparison of pressures using pull-tabs (Non-woven, 71.89 psi)

Radius	Pull-tab stress (psi)			Average	Std. Dev	Confidence 95%	Error \pm
	1	2	3				
2.011	1.819	1.88	1.85	1.850	0.031	0.035	0.017
2.664	2.59	2.528	2.528	2.549	0.036	0.041	0.020
3.495	2.466	2.405	2.466	2.446	0.035	0.040	0.020
4.194	2.312	2.343	2.405	2.353	0.047	0.054	0.027
4.887	2.158	2.22	2.158	2.179	0.036	0.041	0.020

Table 4.7 Error analysis of pressures (Non-woven, 71.89 psi)

4.9 Comparison Of Strains for Non-woven Material

Three trials were done on a same roll with the tabs at specific points. The average of the three trials was done and the errors involved, investigated. The average of the three trials is shown in fig. 4.8. The error involved is shown in table 4.8.

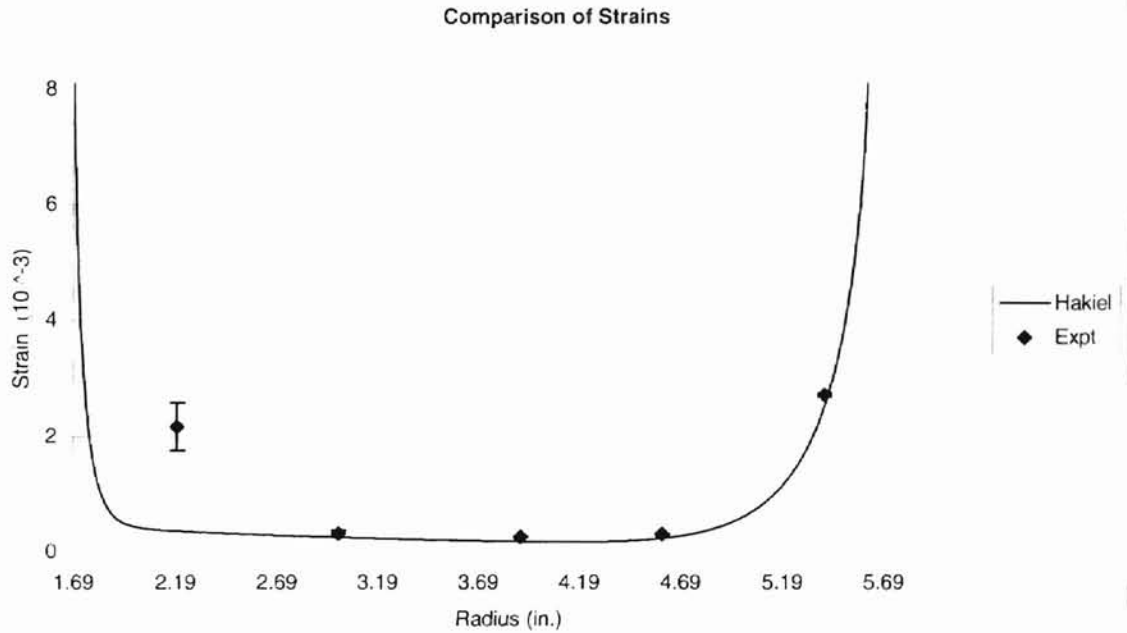


Fig. 4.8 Comparison of strains (Non-woven, 71.89 psi)

Radius	Strain (10 ⁻³)			Average	Std. Dev.	Confidence 95%	Error ±
	1	2	3				
2.2	1.417	2.888	2.196	2.167	0.736	0.833	0.4164
3	0.389	0.189	0.351	0.310	0.106	0.120	0.0601
3.9	0.26	0.238	0.28	0.259	0.021	0.024	0.0119
4.6	0.314	0.278	0.311	0.301	0.020	0.023	0.0113
5.4	2.674	2.694	2.782	2.717	0.057	0.065	0.0325

Table 4.8 Error analysis of strains (Non-woven, 71.89 psi)

Chapter 5

CONCLUSIONS

The objective of this thesis was to determine whether the strains predicted by a theoretical model could be measured in a wound roll. During the course of the investigation, a new method to determine the strains inside a wound roll has been invented. The following conclusions can be drawn from the investigation.

- 1) This method is non-destructive and repeatable when compared to the Cameron gap test method. The same roll can be used to obtain results with variations in parameters like the web tension, speed, etc. Possible errors involved in using different rolls are thus eliminated.
- 2) The method appears to produce theoretically consistent strains for low modulus materials as shown in the case of the LDPE (fig. 4.1 and fig. 4.4) and the non-woven material (fig. 4.8). The 95% confidence interval for LDPE wound at 100 psi at radius of 3.687 in. was 0.38 in/in which is 4.05 psi confidence interval for radial stress as mentioned in section 4.1. According to Fikes work on FSRs at section 2.3.3, the variation in FSR measured values was 16 psi. Hartwig[18] obtained a maximum variation of 5 psi using pull-tabs. But, his confidence interval was obtained at a radial

pressure of 70 psi. Within the pull-tabs' useful range of 0 - 40 psi, his confidence intervals were from 0.09 psi to 3 psi. Pull-tabs are the most accurate means of pressure measurement in wound rolls, with the limitation of a low pressure range (0-70 psi).

- 3) This method can be used to determine the roll-structure even when the interlayer pressures are as high as 190 psi which are measured using FSRs in fig. 4.5. Hence, the method is better than the pull-tab method of determining the roll-structure when the pressures exceed 60 psi.
- 4) The method was shown to be accurate at all points except close to the core with a 6" gage length (fig. 4.1, fig. 4.4, and fig. 4.8). This is due to the fact that the error involved in using a vernier increases as measurements are made closer to the core. The accuracy can be improved by placing the tabs at greater distances than 6" thus making the deformation greater but never allowing a distance larger than the circumference at that radius.
- 5) The method provides output in engineering units which can directly be related to the roll-structure. This method can be used to compare the internal pressures of say, LDPE and non-woven at a particular radius (using fig. 4.2 and fig. 4.7 respectively)
- 6) Density to stress conversions; and hence a reliable roll-structure assessment, according to Roisum[24], should not be made in the regions where the stress to density factor is between $-10E-6$ to $10E-6$ and where the factor is highly nonlinear and changing sign. The circumferential strain method has no such limitations and can be used to structure the roll at any point

Chapter 6

FUTURE WORK

The procedure of measuring the strain using the calipers is a crude one. For LDPE and such low-elastic modulus materials, the strain is very high when compared to the strain of high modulus materials like newsprint for example. Hence some other technique has to be developed for measuring more accurately the strains and the radius. One such set up was developed but is in its initial stages. The set up is explained below.

6.1 Strain measurement with Potentiometer

The equipment consisted of three parts.

1) An aluminum block with a hole for the potentiometer shaft which fits exactly into the core. The aluminum block is as shown below

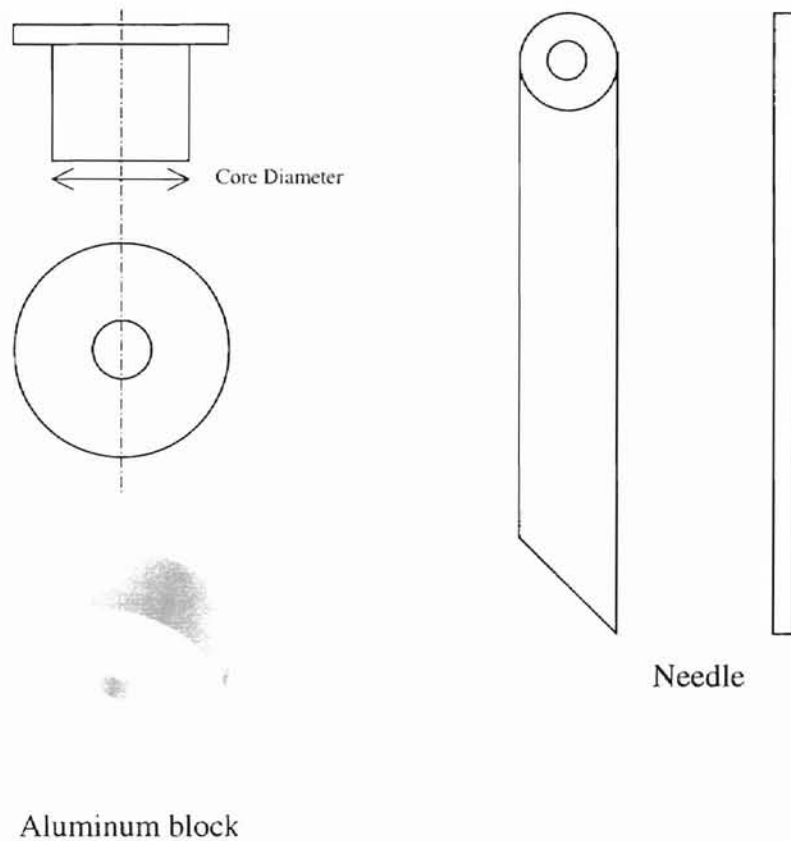


Fig 6.1 Potentiometer set up

The aluminum block was machined very precisely so that it fits into the core without any wobbling which could and will affect the readings.

2) Potentiometer: A very high linearity potentiometer was used to take the angular readings.

3) Needle with ruler: A needle with accurate and straight edges was machined and a ruler of high precision was riveted on it.

The circuit diagram of the set up is as shown below.

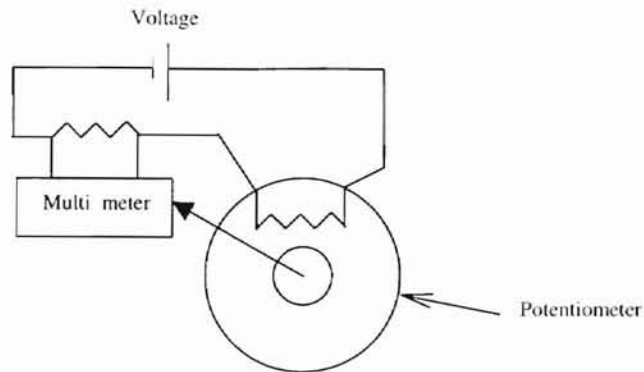


Fig. 6.2 Circuit diagram of potentiometer set up

The needle was interference fitted onto the potentiometer shaft. This was done to prevent any relative movement between the needle and the potentiometer shaft. The hub (aluminum block) was then inserted into the core and the wires were taken from the other side of the core. The circuit connection was made as shown in the circuit diagram above and readings were taken. Constant voltage was supplied using a voltmeter.

When the needle is turned, the potentiometer shaft also turns which in turn increases the resistance of the potentiometer. This change in resistance is displayed as a change in voltage. A calibration curve was obtained which could be used to predict the number of degrees rotation for a particular voltage value

6.2 Calibration

Before using the potentiometer to measure the angle, the potentiometer was calibrated to obtain a curve of angle vs. voltage. This was obtained by marking the 0° position of the potentiometer and noting the voltage. Then the potentiometer was rotated by known angles and the voltages taken.

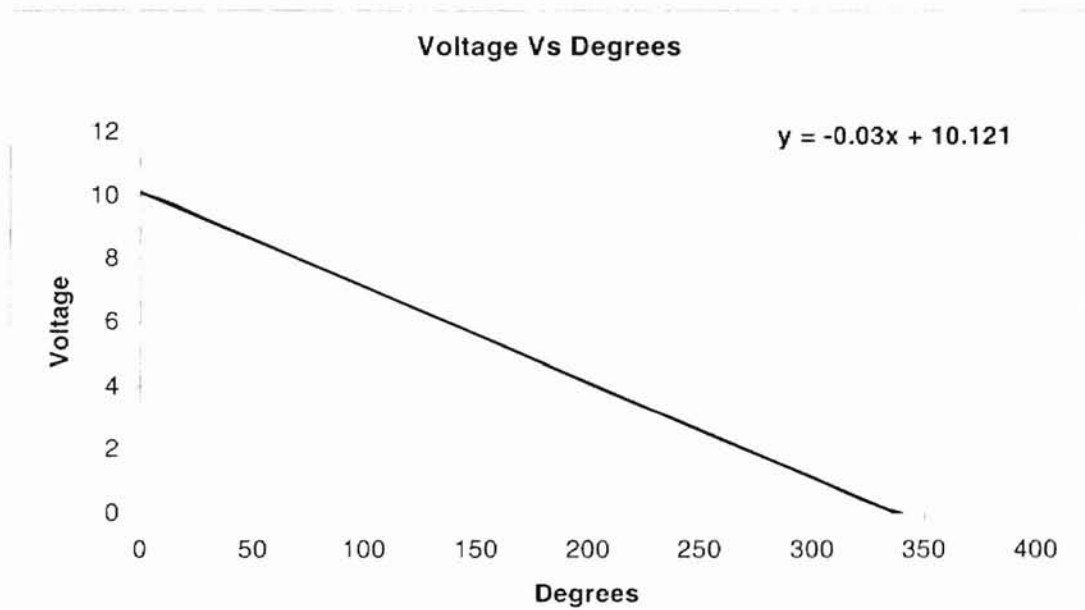


Fig. 6.3 Calibration of Potentiometer

The calibration curve above enabled us to determine the amount of rotation. The ruler on the slider gave us the radius at which the tabs were placed. Using the information and using the arc length formula, the distance of separation between the tabs was determined.

This method was accurate enough for LDPE. But for higher modulus materials, it is still not very accurate. Some other form of measurement has to be discovered. The ruler on the needle is limited in accuracy. The most accurate ruler that we could obtain was a machinist's ruler and the least count was 1/100th of an inch. The ruler was riveted onto the needle using countersunk rivets.

Some other form of precise calculation has to be invented such that the radius can be measured more precisely. Also, a slider could be designed to move on the needle so that it has a projecting end which can come in contact with the tab and then the needle could be moved to make the slider end come in contact with the next tab hence accurately measuring the angle between the tabs. Because of all these limitations, the vernier-caliper was used for all measurements because the radius measurement is one of the most important measurements which determines the strain.

6.3 Tabs

The shim tabs were feasible for strain measurements only due to the reason that low-modulus materials demonstrating high strains were used. In cases where high-modulus materials are adopted, the accuracy is highly dubitable. Also, the process of halting the web in between winding and placing the tab is laborious. A better method to place the tabs has to be invented. But recall that when the roll is being wound, it is in tension. Consequently, strain has already taken place on the web. If tabs are placed on the web, say during running, we are tabbing a pre-strained web. The final strain will be the sum of the two strains; one during winding and the other after its been rolled. Also, due

to the visco-elastic nature of the web, under time dependent loading, the amount of strain is not uniform. Hence, the machine should be in such a modified form to loosen up the web so that there is no strain and there is time for the visco-elastic web to come back to its previous relaxed state and then the tabs should be placed. If the strains are to be added (initial and final), then the amount of strain in the web which is dependent on the radial modulus which in-turn is non-linear, has to be determined accurately.

One other possibility for using the tabs for high-modulus materials is to use a greater distance of separation. But as we increase the distance of separation, the tabs would not be on the same radial layer but on different layers. A template must be developed which will give the exact radius of the tab given its distance of separation. Varying distances of separation could then be used. The distance between the tabs increasing as the radius increases.

Looking at the graphs in the chapter on results, it can be seen that the readings near the core were unsatisfactory. The possible reasons being the inability of the vernier to measure strains closer to the core and the other being the machine induced errors. Changes should be made in the method of measurement using the vernier and using a device with a higher accuracy to measure the radius and the straight line distance. Controlling the machine accurately near the core should be also looked at.

REFERENCES

1. "Roll hardness using the concrete test hammer". TAPPI Useful Methods, UM 402, pp. 64, 1991.
2. Pfeiffer, J.D. "Internal Pressures in a Wound Roll of Paper", TAPPI Journal, Vol. 49, No. 8, Aug 1966.
3. "Cameron test for determining residual strain in paper". TAPPI Useful Methods, UM 506, pp. 127, 1991.
4. Gilmore, W. *et al.*, "A report on Roll defect Terminology". TAPPI CA1228, TAPPI PRESS, Atlanta, 1977.
5. Rand, T. and Eriksson, L.G. "Physical Properties of Newsprint Rolls During Winding, TAPPI Journal, Vol. 56, No.6, pp. 153-156, June 1973.
6. Welp, E.G. and Schoenmeier, H. "Improving roll structure-a research report", TAPPI Journal, Vol. 67, No.4, pp. 70-76, April 1984.
7. Rosium, D. R. "How to measure roll quality", TAPPI Journal, pp. 91-103, October 1988.
8. Hakiel, Z. "Nonlinear model for wound roll stresses". TAPPI Journal, Vol.70, No. 5, pp.113-117, 1987.

9. Good, J.K. and Fikes, M.W.R. "Using FSRs to measure radial pressure in wound rolls." Proceedings of the First international conference on web handling, Oklahoma State University, Stillwater, 1991.
10. Blaedel, K.L. "A design approach to winding a roll of paper", Ph.D. Dissertation, Univ. Wisconsin, 1974.
11. Wolfermann, W. and Schroder, D. "Web Forces and internal tensions for the winding of an Elastic web", Web forces and internal tensions, pp.25-37.
12. Erriksson, L.G., et al., "Measurement of paper roll density during winding", TAPPI Journal, Vol. 66, No. 1, pp. 63-66, 1983.
13. Monk, D.W., Lautner, W.K. and McMullen, J.F. "Internal stresses within rolls of cellophane". TAPPI Journal, Vol.58, No. 8, August 1975.
14. Rosium, D. R. "The Measurement of Web Stresses during roll winding.", Ph.D. Thesis, Department of Mechanical and Aerospace Engineering, Oklahoma State University, Stillwater, 1990.
15. Hussain, S.M. and Farrell, W.R. "Roll winding – Causes, Effects and Cures of Loose Cores in Newsprint.", TAPPI Journal , Vol.58, No. 8, August 1975.
16. Pfeiffer, J.D. "Nip forces and their effects on wound-in tension", TAPPI Journal, Vol. 60, No.2, pp. 115-117, February 1977.
17. Hertzberg, R.W. "Deformation and fracture mechanics of engineering materials. IV edition, pp.216-232, 1996.
18. Hartwig, J.L. "A study of the WOT measurement method", M.S. Thesis, Oklahoma State University, 2000.

19. Jaffar H., Hamad W., Kabore P., and Wang H. "On-line continuous measurement of rolls' coefficient of restitution", Fifth International conference on Web Handling, June 6-9th, 1999.
20. Giachetto R. M., "Tension losses encountered in centerwound rolls, M.S. thesis, Oklahoma State University, 1990.
21. Fikes M.W.R., "The use of Force Sensing Resistors to measure the radial interlayer pressure in wound rolls", M.S. Thesis, Oklahoma State University, May 1990.
22. Qualls W.R., "Hygothermomechanical characterization of viscoelastic centerwound rolls", PhD thesis, pp.90-100, Oklahoma State University, May 1995.
23. Hussain S.M., Farrell W.R. and Gunning J.R. "Most paper in the roll is in unstable condition", Canadian pulp and paper industry, pp. 52-54, Aug 1968.
24. Roisum, D.R., "The mechanics of roll winding", The Beloit corporation, 1-7 pp. 1-7, Feb 27th, 1986.
25. Budinski, K.G., "Engineering Materials", pp.145-189, Fifth edition, Prentics-Hall, 1998.

APPENDIX

In this appendix will be found all the results of the experiments for quick referral and for further data analysis.

Strain Comparison of LDPE

The plots which follow are the set of data obtained for a web tension of 100 psi on LDPE. Three trials were done and all three are presented below. Plots A-1 through A-3 depict the comparison between the Hakiel model strains with the experimentally measured strains. The speed was maintained between 21-24 ft/min. Fig. A-4 shows the error analysis conducted on the three trials and 95% confidence levels have been established.

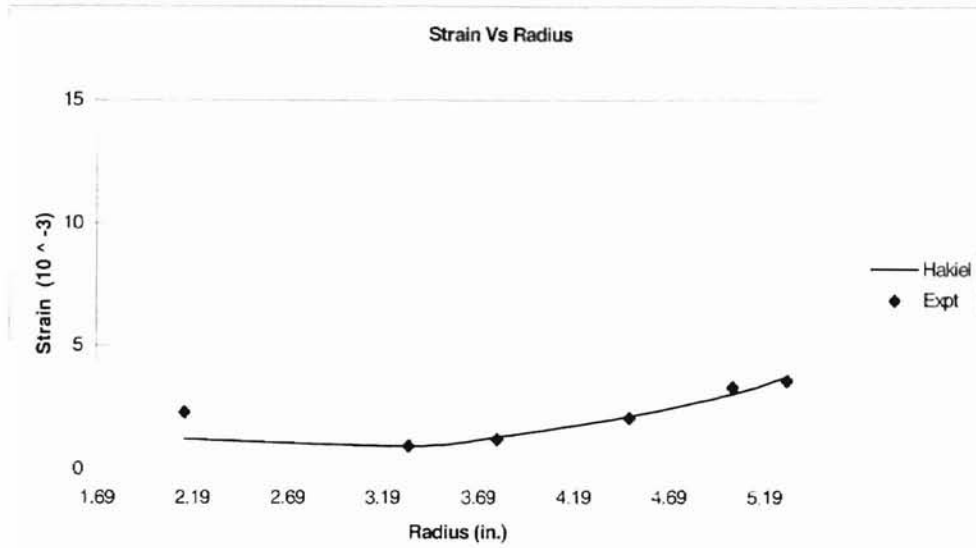


Fig. A-1 Comparison of trains (LDPE, 100 psi, Trial 1)

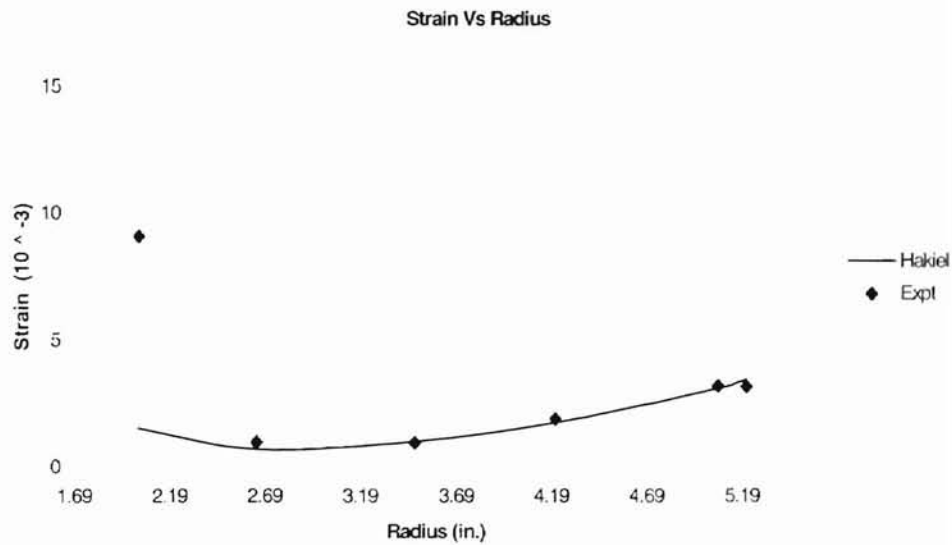


Fig. A-2 Comparison of Strains (LDPE, 100 psi, Trial 2)

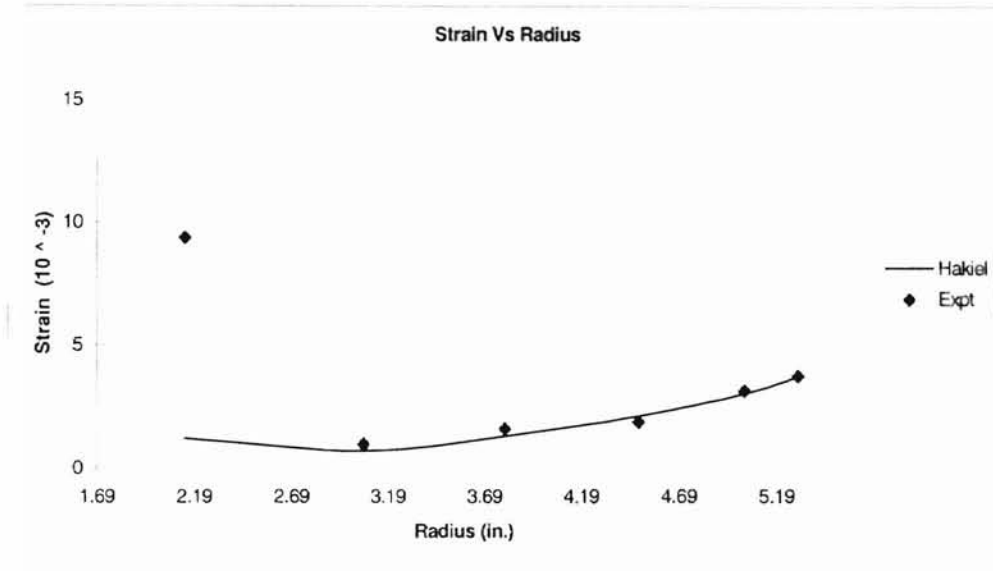


Fig. A-3 Comparison of Strains (LDPE, 100 psi, Trial 3)

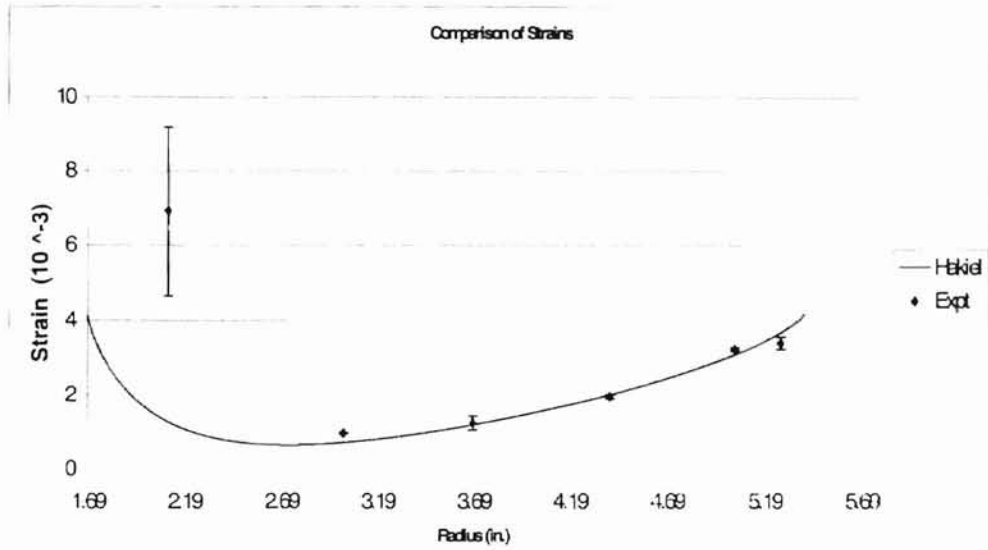


Fig. A-4 Error analysis on strain values (LDPE, 100 psi)

Radius	Strains (10^{-3})			Average	Std. Dev	Confidence 95%	Error \pm
	1	2	3				
2.108	2.292	9.077	9.393	6.921	4.012	4.540	2.270
3.013	0.928	0.975	0.984	0.962	0.030	0.034	0.017
3.687	1.188	0.943	1.605	1.245	0.335	0.379	0.189
4.395	2.063	1.904	1.891	1.953	0.096	0.108	0.054
5.04	3.301	3.211	3.155	3.222	0.074	0.083	0.042
5.275	3.267	3.166	3.73	3.388	0.301	0.340	0.170

Table A-1 Error analysis of Strains (LDPE, 100 Psi web tension)

Pressure Comparison Using Pull-tab For LDPE

Fig. A-5 through A-7 shows the comparison of radial pressures measured using pull-tabs with the Hakiel pressures. The speed was maintained at 20 ft/min and the web tension was 100 psi. Fig. A-8 is the summarized plot showing error bars and 95% confidence levels established.

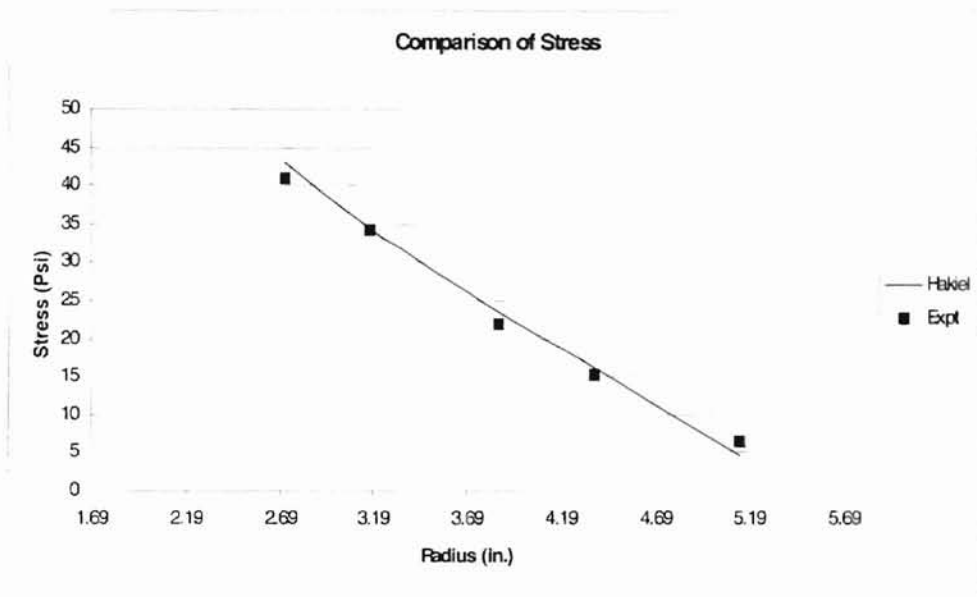


Fig. A-5 Comparison of Stresses using Pull-tabs (LDPE, 100 psi, Trial 1)

Radius in.	Expt. Stress Psi	Hakiel Stress Psi	Pull Force (lb.)		
			1	2	3
2.718	40.86	43.07	120.5	119	122.6
3.168	34.36	34.42	98.1	97.8	99.2
3.86	21.90	23.63	56.5	58.2	58.8
4.368	15.35	16.26	37.6	38.4	38
5.137	6.40	4.67	13.3	13.1	14.2

Avg.	Std Dev	Confidence
		95%
120.70	1.81	2.00
98.37	0.74	0.82
57.83	1.19	1.32
38.00	0.40	0.44
13.53	0.59	0.65

Table A-2 Error analysis of pull-tab readings (LDPE, 100 psi, Trial 1)

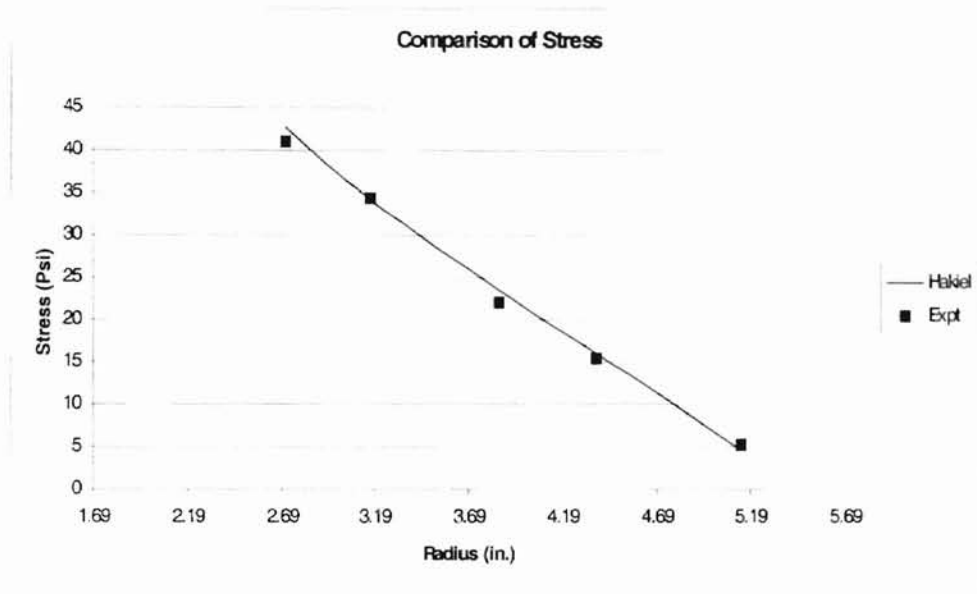


Fig. A-6 Comparison of Stresses using Pull-tabs (LDPE, 100 psi, Trial 2)

Radius in.	Expt. Stress Psi	Hakiel Stress Psi	Pull Force (lb.)		
			1	2	3
2.708	41.14	42.64	120.5	121.5	123
3.162	34.44	34.13	99	99	98
3.854	22.16	23.51	58.6	58	59.3
4.371	15.35	16.05	37	38	39
5.138	5.30	4.48	10.6	10	11.9

Avg.	Std Dev	Confidence
		95%
121.67	1.26	1.39
98.67	0.58	0.64
58.63	0.65	0.72
38.00	1.00	1.11
10.83	0.97	1.08

Table A-3 Error analysis for Pull-tabs stresses (LDPE, 100 psi, Trial 2)

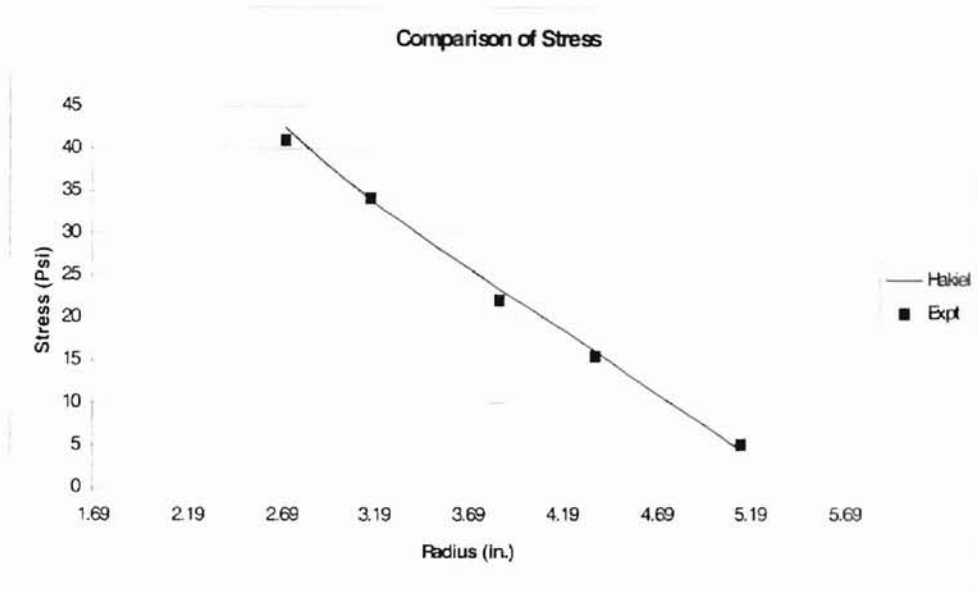


Fig. A-7 Comparison of Stresses using Pull-tabs (LDPE, 100 psi, Trial 3)

Radius in.	Expt. Stress Psi	Hakiel Stress Psi	Pull Force (lb.)		
			1	2	3
2.717	41.04	42.47	121	121	122
3.172	34.15	33.96	97	98	98
3.864	22.13	23.36	58.5	58.2	58.9
4.37	15.40	16.08	38	37.5	39
5.142	4.92	4.42	10	9.8	10

Avg.	Std Dev	Confidence	% Error
		95%	
121.33	0.58	0.64	3.4
97.67	0.58	0.64	0.6
58.53	0.35	0.39	5.3
38.17	0.76	0.85	4.2
9.93	0.12	0.13	11.4

Table A-4 Error analysis of Pull-tab stresses (LDPE, 100 psi, Trial 3)

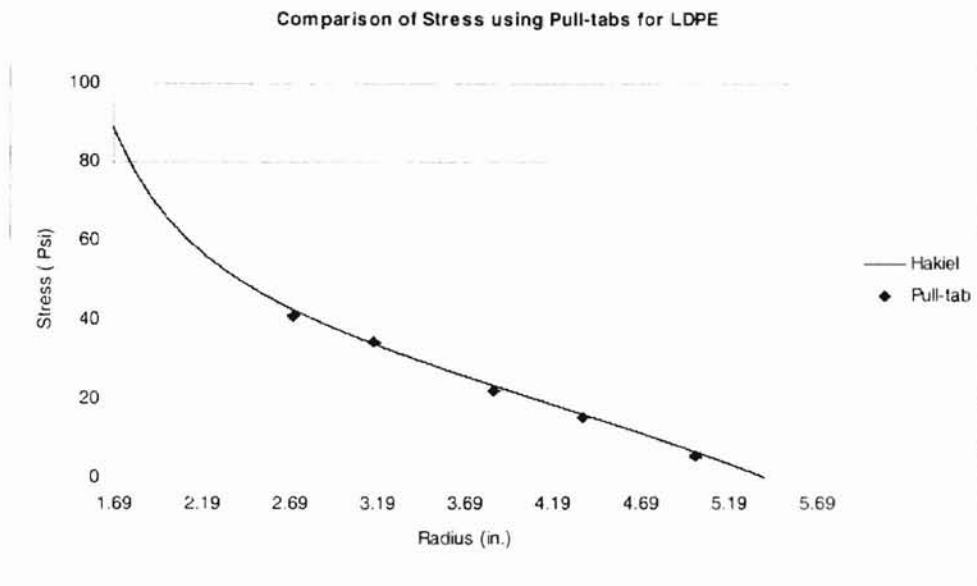


Fig. A-8 Error analysis on three pressures (LDPE, 100 psi)

Radius	Pull-tab stress (Psi)			Average	Std. Dev	Confidence	Error ±
	1	2	3				
2.714	40.86	41.14	41.04	41.013	0.142	95%	0.080
3.167	34.36	34.44	34.15	34.317	0.150	0.169	0.085
3.859	21.9	22.16	22.13	22.063	0.142	0.161	0.080
4.369	15.35	15.35	15.4	15.367	0.029	0.033	0.016
5.139	6.4	5.3	4.92	5.540	0.769	0.870	0.435

Table A-5 Error Analysis of Pull-tab Pressures (LDPE, 100 psi)

Pressure Comparison Using FSRs For LDPE

Plots A-9 through A-11 denote the comparison of pressures using FSR with Hakiel's model generated pressures. Three trials were done even in this case where the speed was maintained between 20 – 23 ft/min. Fig. A-12 displays the error bars along with 95% confidence level established.

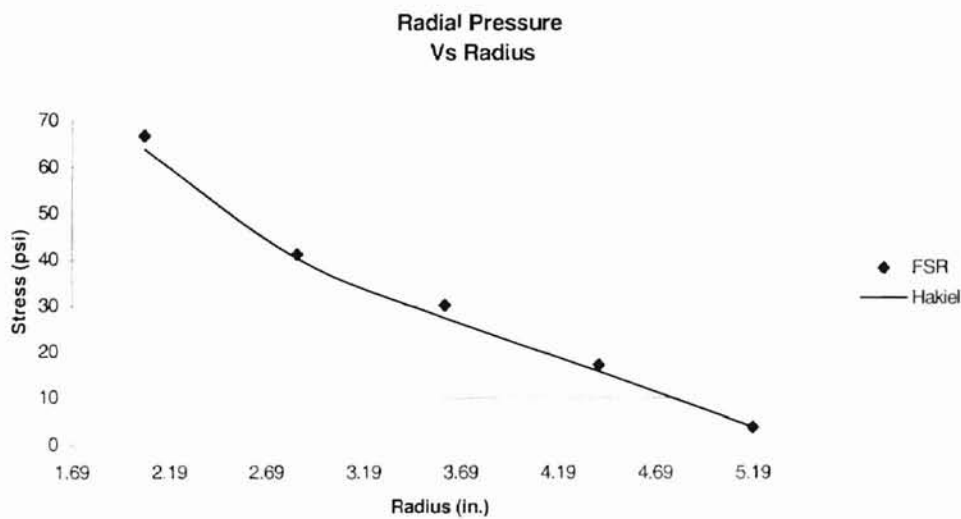


Fig. A-9 Comparison of Pressures using FSR (LDPE, 100 psi, Trial 1)

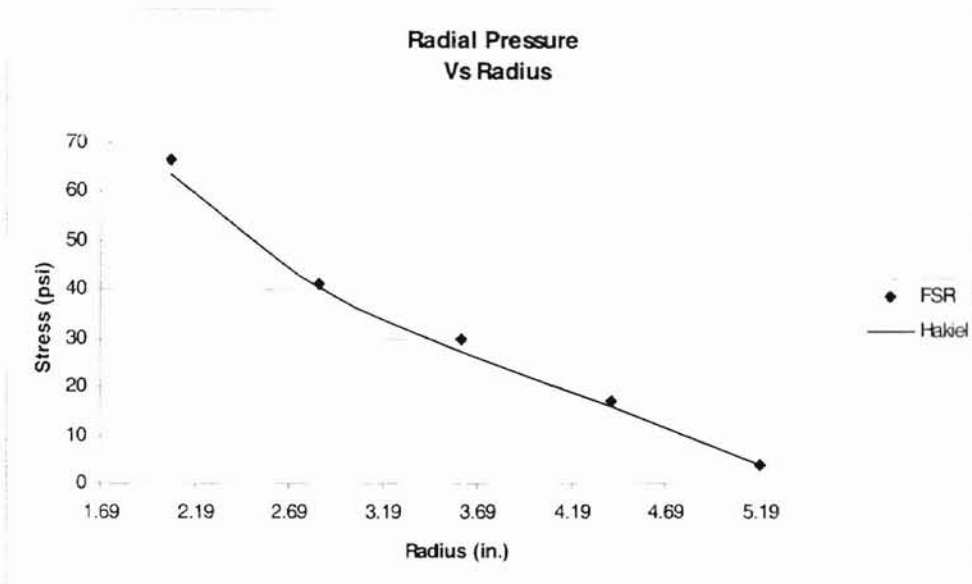


Fig. A-10 Comparison of Pressures using FSR (LDPE, 100 psi, Trial 2)

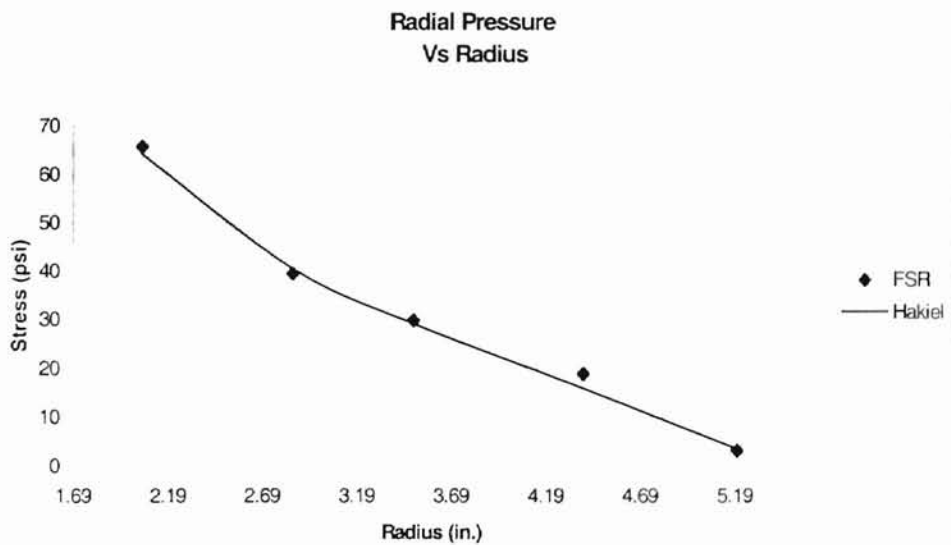


Fig. A-11 Comparison of Pressures using FSR (LDPE, 100 psi, Trial 3)

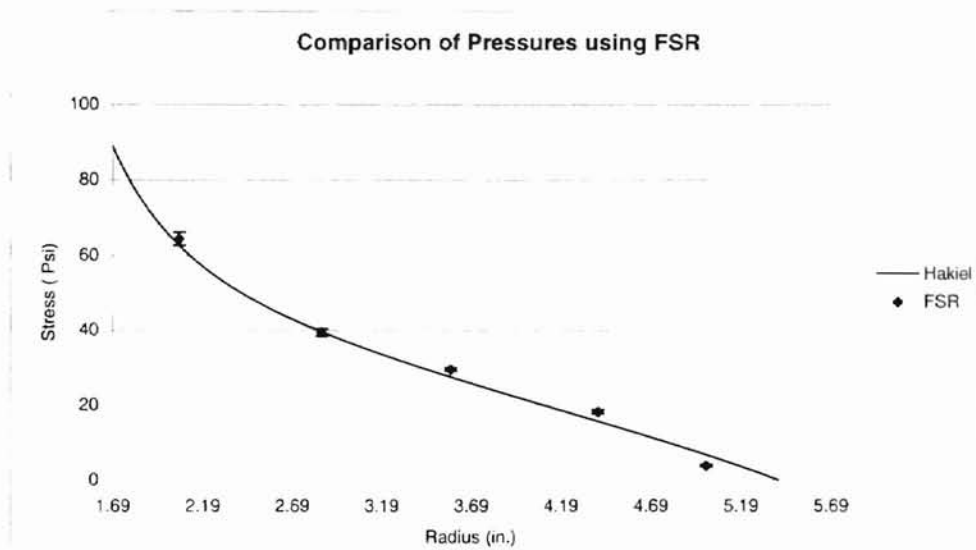


Fig. A-12 Error Analysis of three FSR readings (LDPE, 100 psi)

Radius	FSR stress (Psi)			Average	Std. Dev	Confidence 95%	Error ±
	1	2	3				
2.059	66.65	60.87	65.75	64.423	3.110	3.519	1.760
2.852	41.22	37.72	39.55	39.497	1.751	1.981	0.990
3.577	30.08	28.66	29.89	29.543	0.771	0.872	0.436
4.398	17.17	18.5	18.88	18.183	0.898	1.016	0.508
5.2	3.85	4.35	3.2	3.800	0.577	0.653	0.326

Table A-6 Error analysis for three FSR trials (LDPE, 100 psi)

Strain comparison For LDPE

Plots A-13 through A-15 shows the comparison of strains obtained experimentally with the Hakiel strains. The web tension was 200 psi and the speed was maintained between 20-23 ft/min. Three trials were conducted and the error analysis on the three trials is shown in plot A-16 along with the 95% confidence level established.

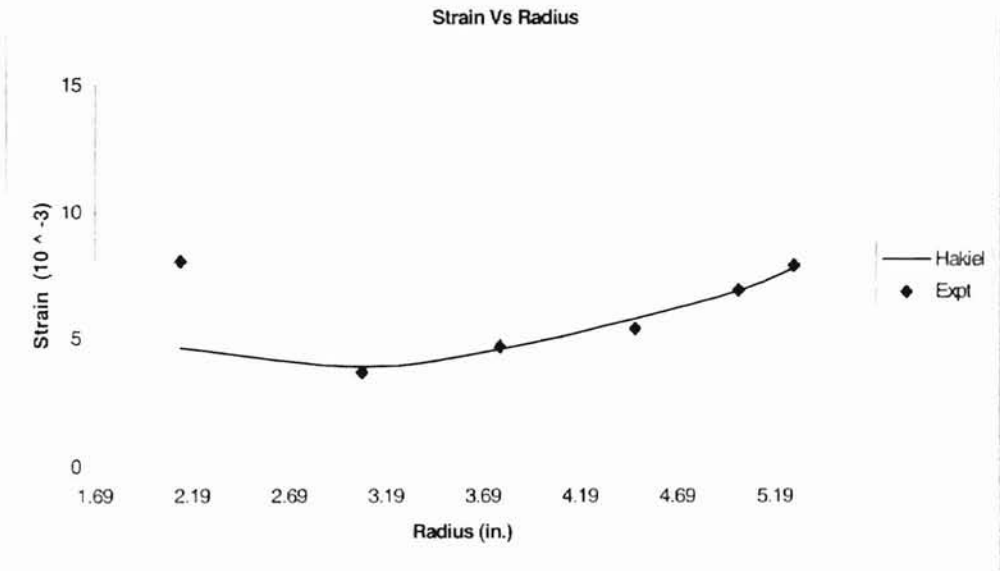


Fig. A-13 Comparison of Strains (LDPE, 200 psi, Trial 1)

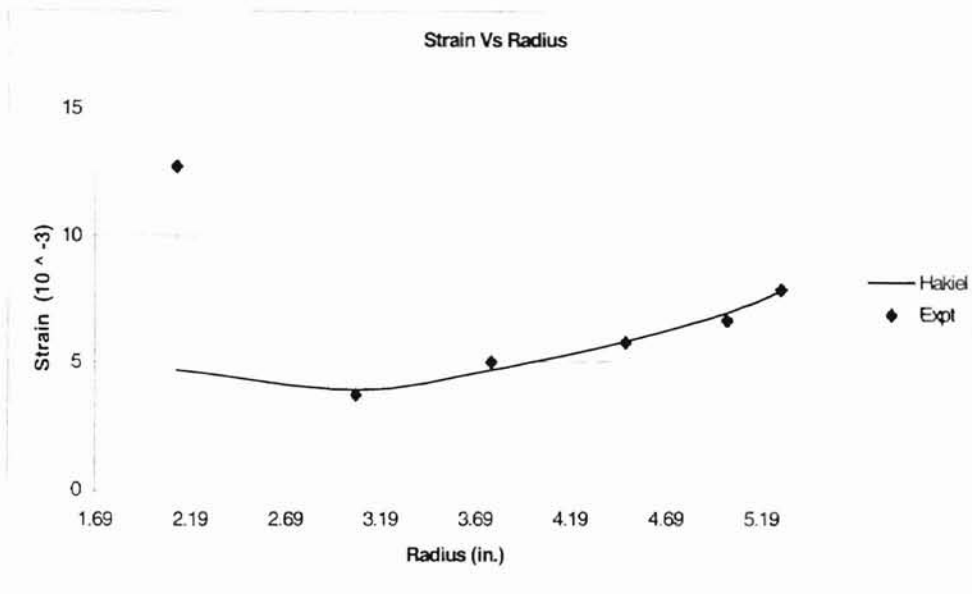


Fig. A-14 Comparison of Strains (LDPE, 200 psi, Trial 2)

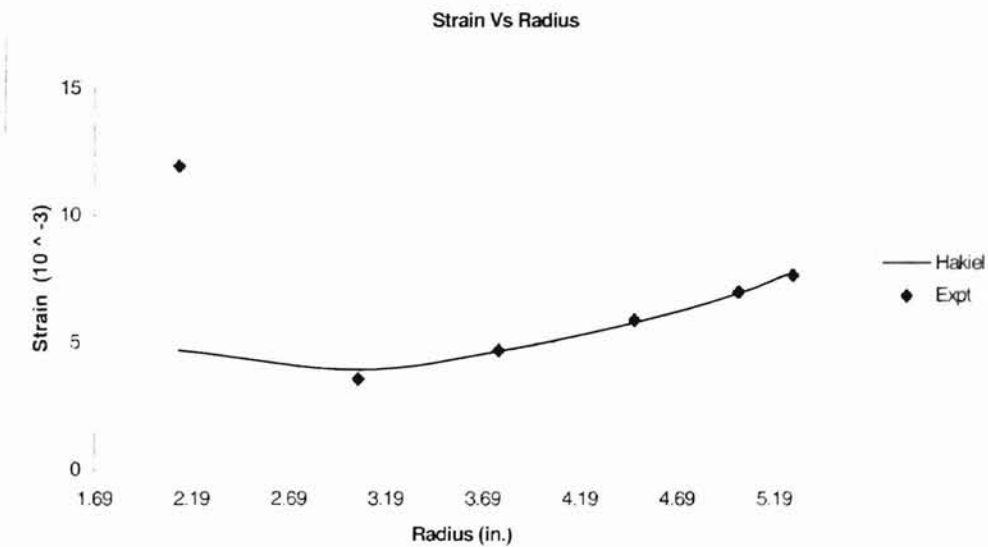


Fig. A-15 Comparison of Strains(LDPE, 200 psi, Trial 3)

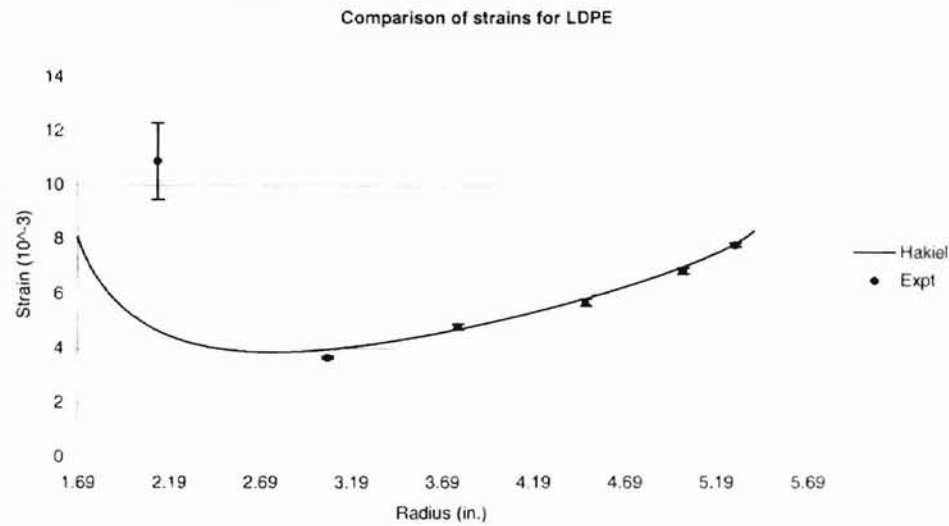


Fig. A-16 Error analysis of strains for three trials (LDPE, 200 psi)

Radius	Strain (10 ⁻³)			Average	Std dev	Confidence 95%	Error ±
	1	2	3				
2.127	8.063	12.722	11.928	10.904	2.492	2.820	1.410
3.06	3.689	3.725	3.575	3.663	0.078	0.089	0.044
3.776	4.701	5.004	4.678	4.794	0.182	0.206	0.103
4.475	5.409	5.758	5.878	5.682	0.244	0.276	0.138
5.007	6.925	6.609	6.982	6.839	0.201	0.227	0.114
5.291	7.902	7.831	7.649	7.794	0.130	0.148	0.074

Table A-7 Error Analysis of three Strains (LDPE, 200 Psi)

Pressure Comparison Using FSRs For LDPE

Plots A-17 through A-19 show the comparison of pressures obtained using FSRs with the Hakiel pressures for LDPE wound at 200 psi web tension. Pull-tabs were not used in this case since the pressures in a wound roll far exceeded the pull-tab useful range. Three trials were run and the pressures obtained using the FSRs were tabulated. The error analysis on the three readings was done and 95% confidence levels established. This is shown in Fig. A-20.

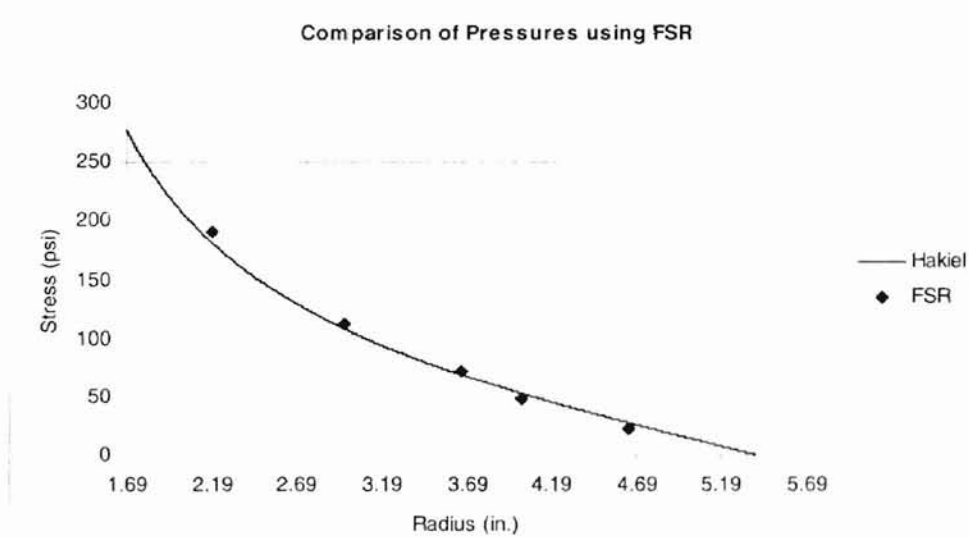


Fig. A-17 Comparison of Pressures (LDPE, 200 psi, Trial 1)

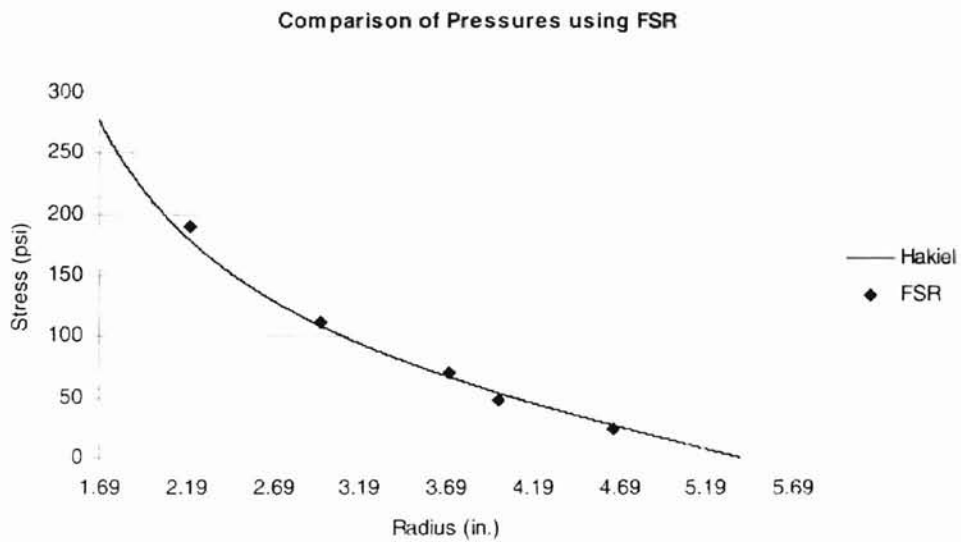


Fig. A-18 Comparison of Pressures (LDPE, 200 psi, Trial 2)

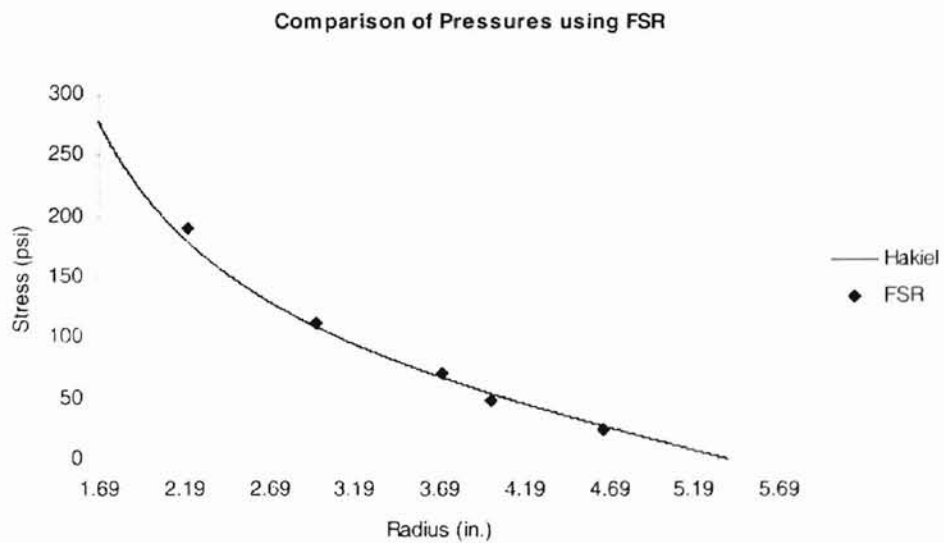


Fig. A-19 Comparison of pressures (LDPE, 200 psi, Trial 3)

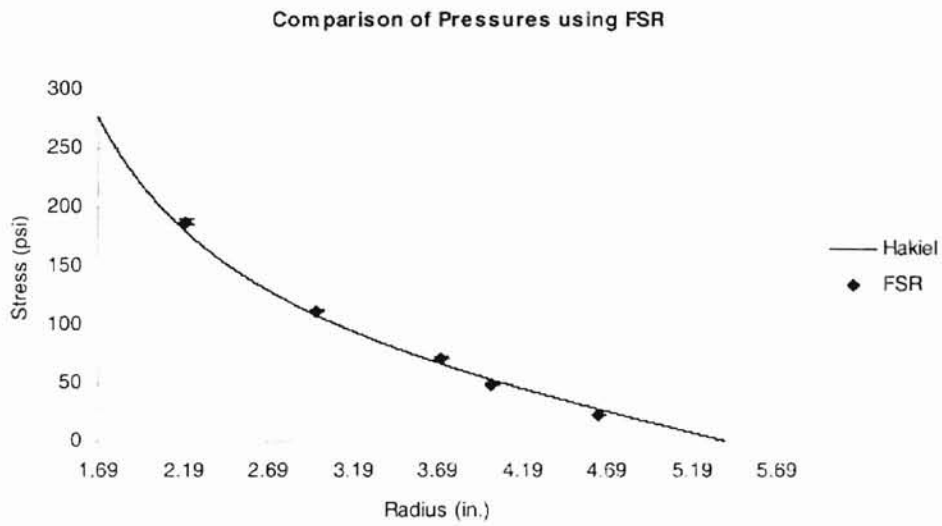


Fig. A-20 Comparison of pressures of three trials (LDPE, 200 psi)

Radius	Stresses (Psi)			Average Psi	Std.dev	Confidence 95%	Error \pm
	1	2	3				
2.20	190.40	189.20	183.10	187.57	3.91	4.43	2.21
2.98	112.60	112.40	110.20	111.73	1.33	1.51	0.75
3.71	71.90	70.20	72.60	71.57	1.23	1.40	0.70
4.01	48.70	47.90	50.90	49.17	1.55	1.76	0.88
4.65	22.90	23.50	22.60	23.00	0.46	0.52	0.26

Table A-8 Error analysis of three FSR pressures (200 psi, LDPE)

Non-woven web (Strain comparison)

Plots A-21 through A-23 denote the comparison of the experimentally measured strains with the Hakiel derived strains. Three winds were done at 71.89 psi in this case and the error analysis of the three trials is shown in Fig. A-24.

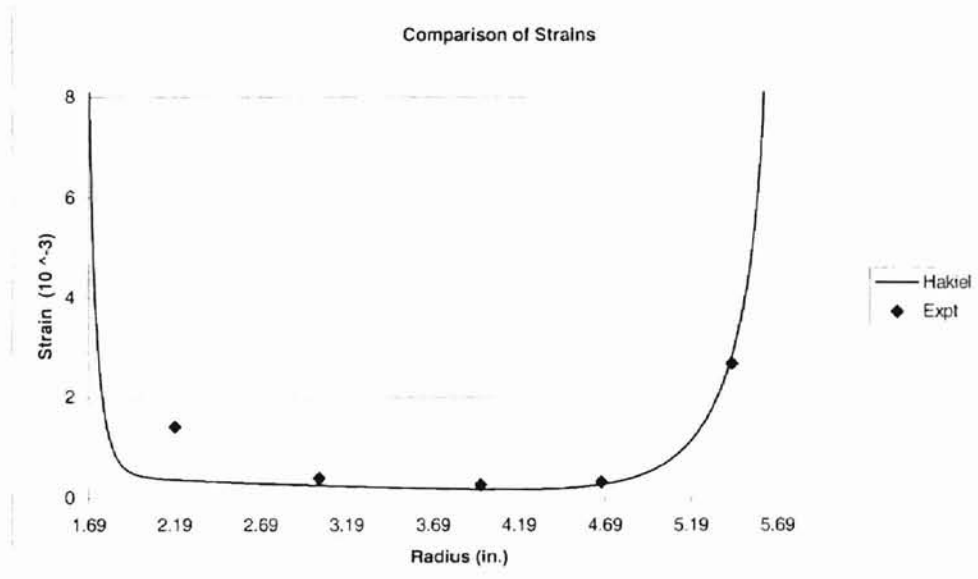


Fig. A-21 Comparison of strains (Non-woven, 71.89 psi, Trial 1)

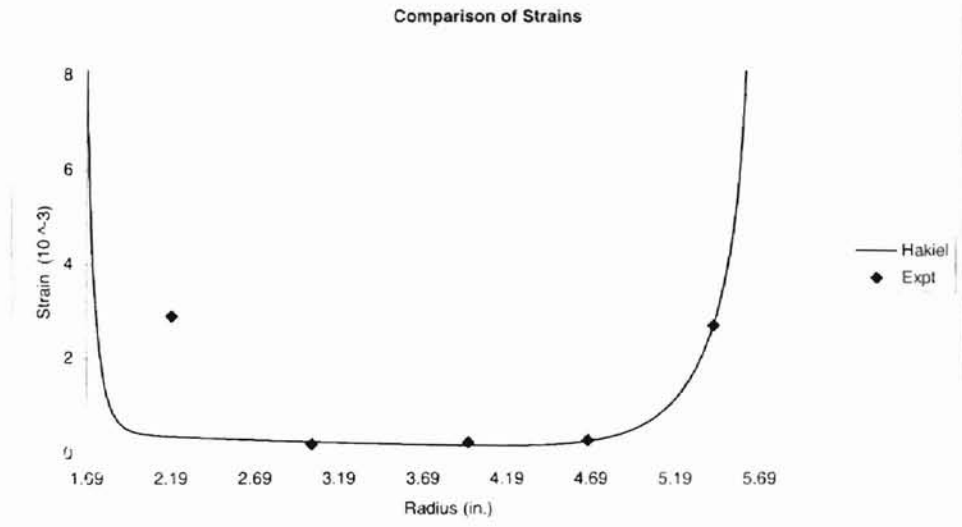


Fig. A-22 Comparison of Strains (Non-woven, 71.89 psi, Trial 2)

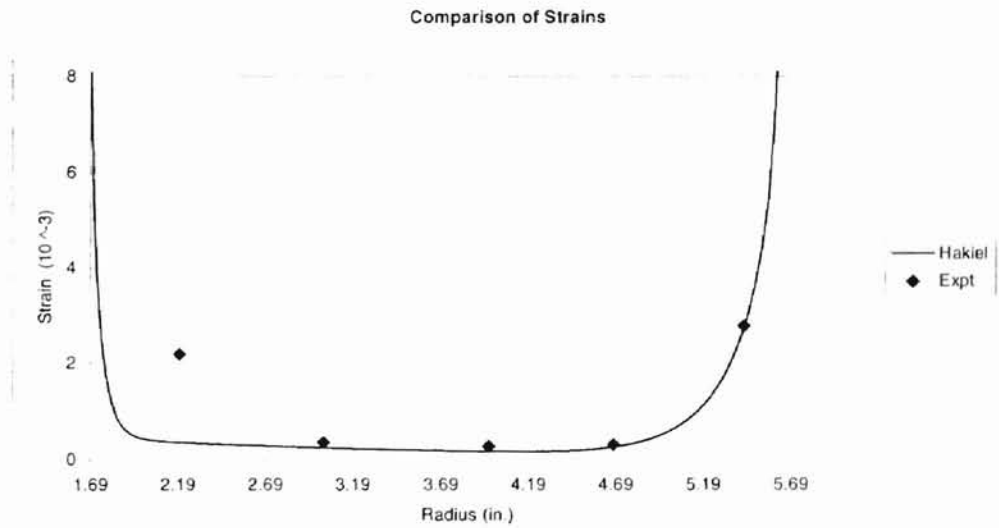


Fig. A-23 Comparison of Strains (Non-woven, 71.89 psi, Trial 3)

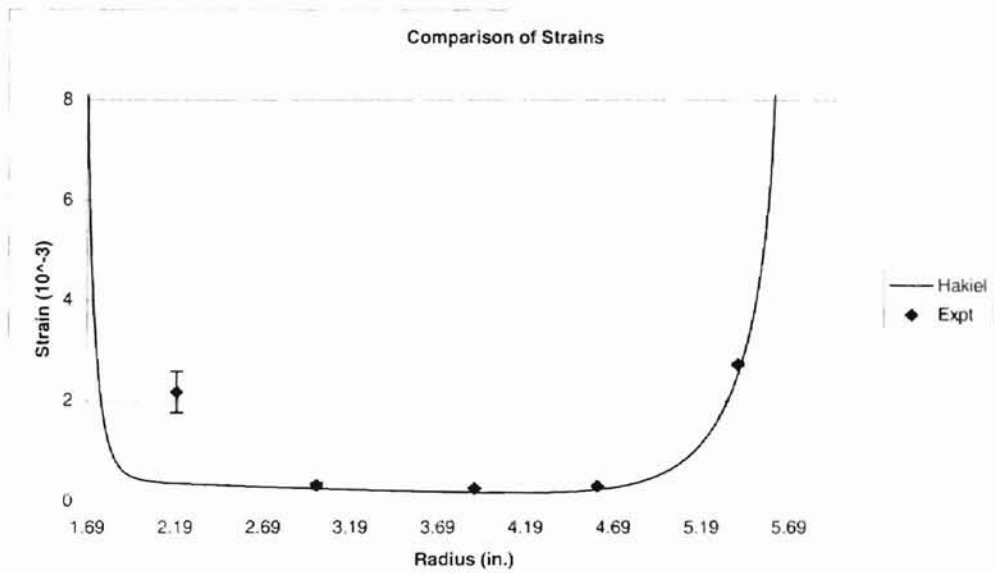


Fig. A-24 Error analysis on three strains (Non-woven, 71.89 psi)

Radius	Strain (10^{-3})			Average	Std dev.	Confidence 95%	Error Bar \pm
	1	2	3				
2.2	1.417	2.888	2.196	2.167	0.736	0.833	0.416
3	0.389	0.189	0.351	0.310	0.106	0.120	0.060
3.9	0.26	0.238	0.28	0.259	0.021	0.024	0.012
4.6	0.314	0.278	0.311	0.301	0.020	0.023	0.011
5.4	2.674	2.694	2.782	2.717	0.057	0.065	0.033

Table A-9 Error analysis on three strains (Non-woven, 71.89 psi)

Non-Woven (Stress comparison using Pull-tabs)

The comparison of pressures in the non-woven web was done using pull-tabs wound at 71.89 psi. Three pulls were done on a single pull-tab and three windings were repeated in this fashion. Plots A-25 through A-27 show these results. The resulting nine readings were used to determine the 95% confidence intervals. This is shown in Fig. A-28.

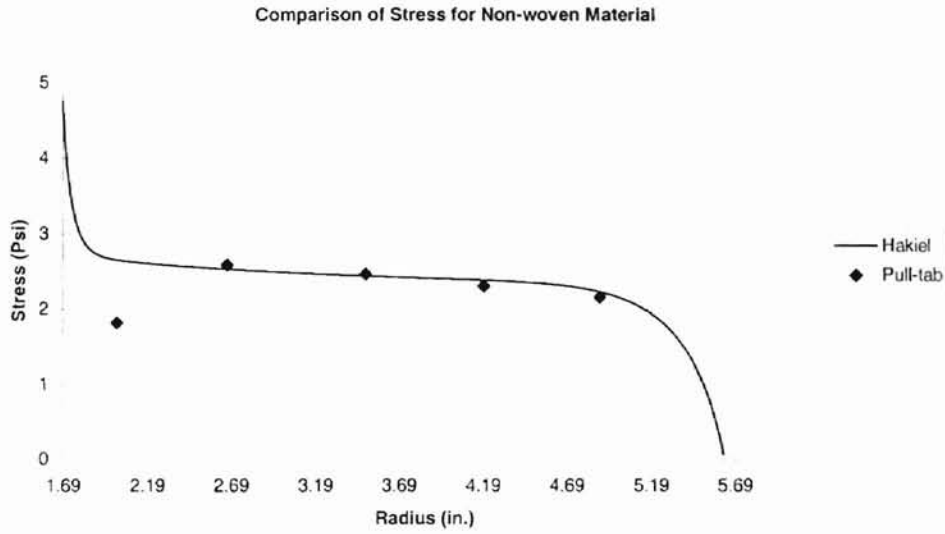


Fig. A-25 Comparison of stresses (Non-woven, 71.89 psi, Trial 1)

Radius	Pull-tab Stress	Hak stress(Psi)	Pull force (lb.)			Average	Std. Dev	Confidence 95%
			1	2	3			
1.69	Psi	4.749						
2.012	1.819	2.653	1.8	1.8	1.8	1.800	0.000	N/a
2.667	2.590	2.529	2.5	2.8	2.6	2.633	0.153	0.173
3.492	2.466	2.441	2.6	2.5	2.4	2.500	0.100	0.113
4.197	2.312	2.385	2.3	2.3	2.4	2.333	0.058	0.065
4.887	2.158	2.229	2.2	2.2	2.1	2.167	0.058	0.065

Table A-10 Comparison of stresses (Non-woven, 71.89 psi, Trial 1)

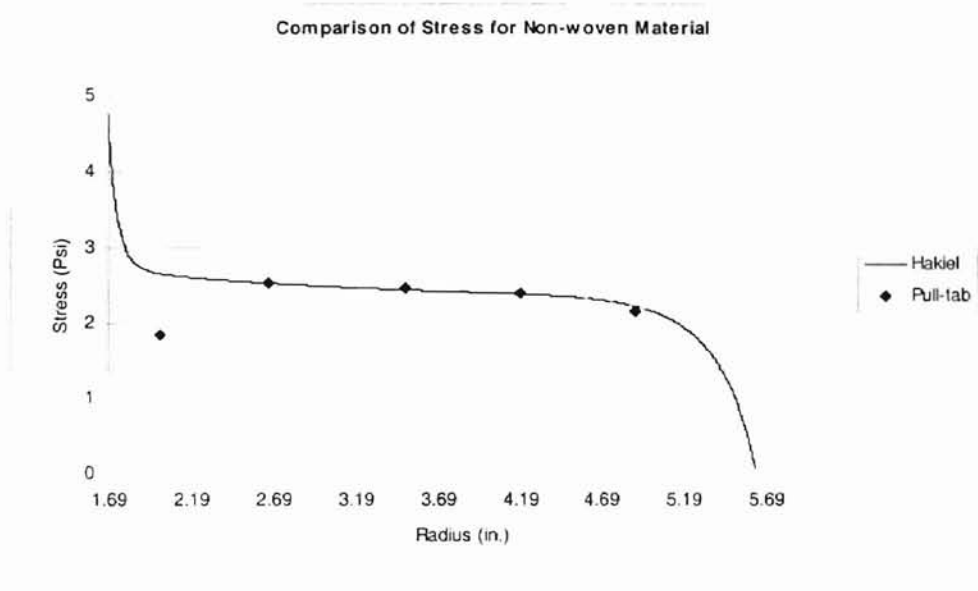


Fig. A-26 Comparison of stresses (Non-woven, 71.89 psi, Trial 2)

Radius	Pull-tab Stress Psi	Hak stress(Psi)	Pull force (lb.)			Average	Std. Dev	Confidence
			1	2	3			
								95%
2.015	1.880	2.653	1.9	1.9	1.8	1.867	0.058	N/a
2.662	2.528	2.530	2.5	2.6	2.6	2.567	0.058	0.065
3.495	2.405	2.441	2.5	2.4	2.4	2.433	0.058	0.065
4.195	2.343	2.385	2.3	2.4	2.4	2.367	0.058	0.065
4.884	2.220	2.229	2.2	2.3	2.2	2.233	0.058	0.065

Table A-11 Comparison of stresses (Non-woven, 71.89 psi, Trial 2)

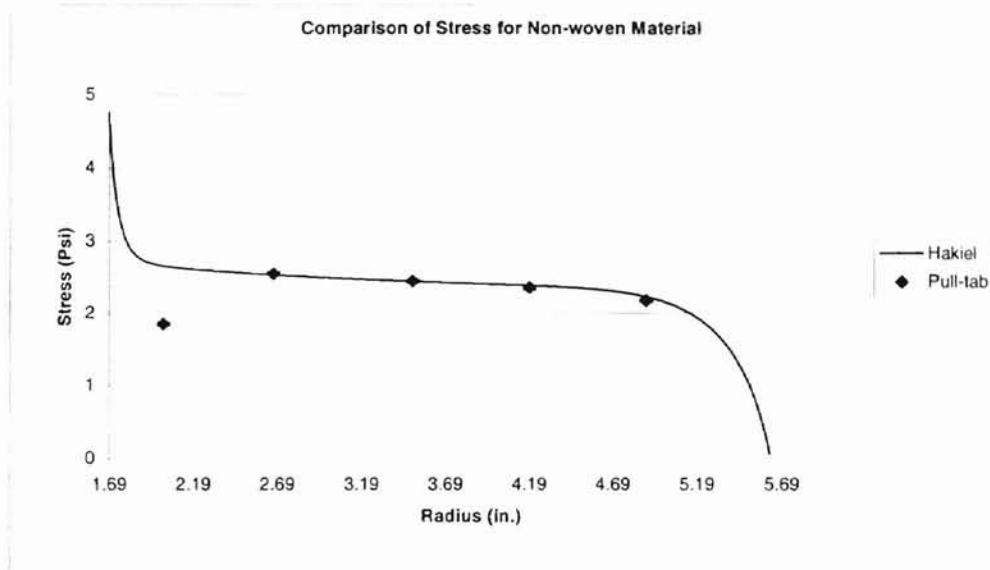


Fig. A-27 Comparison of stresses (Non-woven, 71.89 psi, Trial 3)

Radius	Pull-tab Stress	Hak stress(Psi)	Pull force (lb.)			Average	Std. Dev	Confidence
			1	2	3			
	Psi							95%
2.008	1.850	2.657	1.8	1.9	1.8	1.83	0.06	N/a
2.665	2.528	2.529	2.5	2.6	2.6	2.57	0.06	0.07
3.5	2.466	2.440	2.6	2.5	2.4	2.50	0.10	0.11
4.192	2.405	2.386	2.4	2.5	2.4	2.43	0.06	0.07
4.891	2.158	2.226	2.2	2.1	2.2	2.17	0.06	0.07

Table A-12 Comparison of stresses (Non-woven, 71.89 psi, Trial 3)

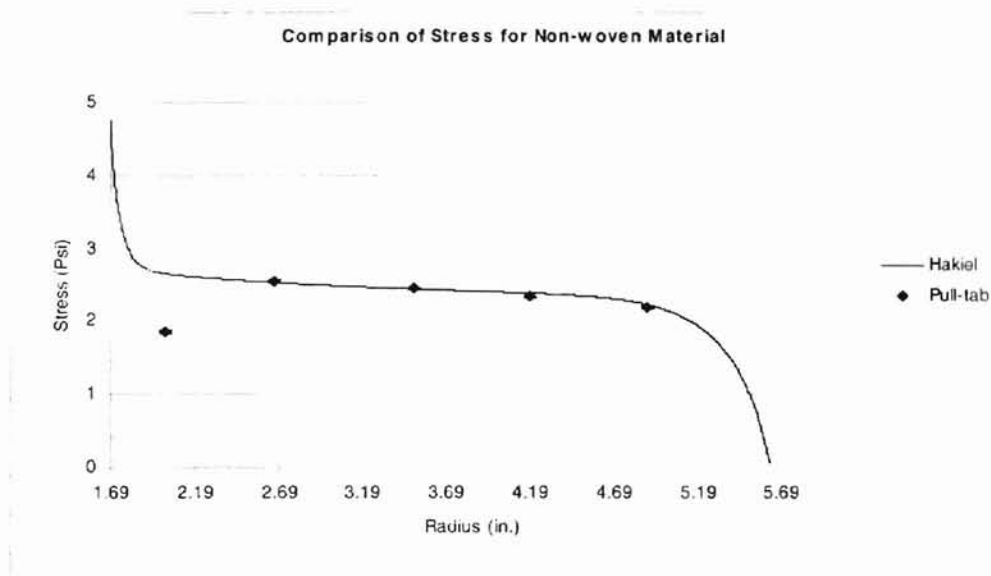


Fig. A-28 Comparison of three stresses (Non-woven, 71.89 psi)

Radius	Pull-tab stress			Average	Std. Dev	Confidence	Error \pm
	1	2	3				
2.011	1.819	1.88	1.85	1.850	0.031	0.035	0.017
2.664	2.59	2.528	2.528	2.549	0.036	0.041	0.020
3.495	2.466	2.405	2.466	2.446	0.035	0.040	0.020
4.194	2.312	2.343	2.405	2.353	0.047	0.054	0.027
4.887	2.158	2.22	2.158	2.179	0.036	0.041	0.020

Table A-13 Error analysis for Pull-tab stresses (Non-woven, 71.89 psi)

Core Property	Value
Core	Carbon Steel
Outside diameter	1.69
Modulus	30,000,000 psi.
Thermal Expn. Coefficient	0

Table A-14 Core Properties

Property	Value
Material	Low Density PolyEthylene
Radial Modulus	$167.24 P - 0.09855 P^2 - 0.000422 P^3$ psi.
Poisson's ratio	0.01
Tangential Modulus	24000 psi.
Caliper	2 mil
RMS	20 μ in.
Kinetic COF web to web	0.21
Kinetic COF web to roller	0.15
Static COF web to web	0.25

Table A-15 Properties for the winder software for LDPE

Property	Value
Material	Non-woven
Radial Modulus	$4.0834 P + 2.8251 P^2 - 0.3089 P^3$ psi.
Poisson's ratio	0.01
Tangential Modulus	8000 psi.
Caliper	5 mil (0.005 in.)
RMS	675 μ in.
Kinetic COF web to web	0.3684
Kinetic COF web to roller	0.2463
Static COF web to web	0.6259

Table A-16 Properties of Non-woven for Winder software

VITA

Sreeram Krishna

Candidate for the Degree of

Master of Science

Thesis: **STUDY OF WEB STRUCTURE USING STRAIN MEASUREMENTS**

Major Field: Mechanical Engineering

Biographical:

Personal Data: Born in Gudiyattam, India, on April 8, 1976, the son of Shri. Krishna, V. and Smt. Narmada Krishna.

Education: Received Bachelor of Engineering Degree in Mechanical Engineering from R.V.College of Engineering, Bangalore University, India in October, 1997. Completed the requirements for Master of Science Degree with a major in Mechanical Engineering at Oklahoma State University in December, 2000.

Experience: Worked in the Indian Institute of Science, Bangalore, India as a Research Assistant in the Mechanical Engineering Department.
Worked as a Teaching Assistant for Dr. Price and Dr. Good in Mechanical and Aerospace Engineering, Oklahoma State University.
Worked as a Research Assistant in the Web Handling Research Center (WHRC), Oklahoma State University, from May 99 to present.